A stochastic RNA editing process targets a limited number of sites in individual *Drosophila* glutamatergic motoneurons

Andrés B. Crane, Suresh K. Jetti, J. Troy Littleton

The Picower Institute for Learning and Memory, Department of Brain and Cognitive Sciences, Department of Biology, Massachusetts Institute of Technology, Cambridge, MA 02139

Correspondence and requests for materials should be addressed to J.T.L. (troy@mit.edu).

Abstract

RNA editing is a post-transcriptional source of protein diversity and occurs across the animal kingdom. Given the complete profile of mRNA targets and their editing rate in individual cells is unclear, we analyzed single cell RNA transcriptomes from *Drosophila* larval tonic and phasic glutamatergic motoneuron subtypes to determine the most highly edited targets and identify cell-type specific editing. From ~15,000 genes encoded in the genome, 316 high confidence A-to-I canonical RNA edit sites were identified, with 102 causing missense amino acid changes in proteins regulating membrane excitability, synaptic transmission, and cellular function. Some sites showed 100% editing in single neurons as observed with mRNAs encoding mammalian AMPA receptors. However, most sites were edited at lower levels and generated variable expression of edited and unedited mRNAs within individual neurons. Together, these data provide insights into how the RNA editing landscape alters protein function to modulate the properties of two well-characterized neuronal populations in *Drosophila*.

Introduction

RNA editing modifies single nucleotides in precursor mRNA (pre-mRNA). The majority of editing is catalyzed by ADARs (adenosine deaminase acting on RNA), a protein family that binds double stranded regions of pre-mRNA during RNA processing and irreversibly deaminates specific adenosines into inosines (A-to-I editing)[1–3]. Edits within coding exons can alter the resulting amino acid sequence as ribosomes recognize inosines as guanines during mRNA translation. In addition, editing of 5' or 3' untranslated (UTR) exons can regulate mRNA splicing, translation and stability[2,4–12]. The level of editing (the fraction of total mRNA in an individual cell with a specific edit) depends on editing site, developmental stage and cell type[13–21]. Although RNA editing is observed across the animal kingdom and occurs in diverse cell types, it is particularly robust in neurons where it regulates excitability and synaptic function[22–27].

Millions of RNA editing sites have been identified in humans, though their significance is obscured as over 95% occur in *Alu* elements, non-coding mobile DNA retroelements that comprise ~11% of the human genome[28–31]. However, aberrant editing of mRNAs encoding ion channels is associated with several neurological conditions in humans[32–36]. A major role for RNA editing in mammalian neurons is the substitution of a glutamine (E) by an arginine (R) residue in the AMPA GluR2 receptor subunit that controls the channel's Ca^{2+} permeability[37,38]. Lack of editing at this site leads to postembryonic lethality and excitotoxic neuronal cell death[26], while exogenous expression of an edited AMPA receptor can rescue neuronal degeneration in *ADAR2*$^{-/-}$ mice[39,40]. Aberrant editing of human GluR2 is linked to disorders such as ALS[41,42]. Mutations in the sole *Adar* gene in *Drosophila melanogaster* cause reduced viability, with surviving adults displaying behavioral dysfunction, temperature-dependent seizures and neurodegeneration[24,25,43–46]. As such, RNA editing has important impacts on neuronal function across invertebrates and vertebrates.

Thousands of RNA editing sites have been previously identified in *Drosophila* using pooled RNA samples from whole animal or brain homogenates, enriched GFP-labeled cell populations obtained by flow cytometry, or based on computational predications of intron-exon base pairing[12,13,16,19,23,47–50]. While sensitivity is increased by combining RNA from many cells, information about cell-to-cell variations in editing levels is lost. In addition, cell-type information about each edit site is determined after the fact or unknown. To examine the landscape and function of RNA editing more systematically, we sought to define the editing profile for two well-characterized neuronal subtypes. *Drosophila* larval motoneurons are commonly used to study

neuronal development and glutamatergic synapse biology[51]. With multiple imaging and electrophysiology toolkits, combined with GAL4 drivers for motoneuron subtypes[52,53], *Drosophila* larvae provide an attractive system for examining impacts of specific RNA editing events[27,54]. Two glutamatergic motoneuron subtypes innervate most larval bodywall muscles. Tonic-like Ib neurons target single muscles and form weaker presynaptic active zones (AZs) that display synaptic facilitation, while phasic Is-like neurons synapse onto multiple muscles and form stronger AZs that undergo synaptic depression[55–62]. These neuronal subtypes also have diverse biophysical and morphological features[63], providing an opportunity to identify the major targets for RNA editing and cell-type specific edits that contribute to their functional properties.

We recently determined the transcriptomes for larval Ib and Is motoneuron subtypes by performing single cell Patch-seq RNA profiling from hundreds of individual Ib and Is neurons[61]. This allowed identification of differentially expressed genes (DEGs) that contribute to the unique properties of these neurons. In the current study, we extend this analysis to define the RNA editing landscape and single cell editing rules for these neuronal populations. These experiments identify the major targets for RNA editing in the two cell types and reveal a highly stochastic RNA editing process that occurs in individual motoneurons across both populations.

Results

RNA editing in larval motoneurons induces missense amino acid changes in a limited number of target proteins

Canonical RNA editing occurs when ADAR deaminates adenosines, converting them into inosines that are interpreted as guanosine by the translation machinery (Fig. 1A). To determine specific sites that are edited in *Drosophila* 3rd instar larval motoneuron subpopulations, we analyzed single cell RNA sequencing data obtained by Patch-seq profiling from 105 individual MN1-Ib (hereafter referred to as Ib) and 101 individual MNISN-Is (hereafter referred to as Is) motoneurons labeled with GFP using GAL4 drivers specific to each cell type[61]. Candidate RNA editing sites were examined by comparing genomic DNA sequenced from parental strains to their single cell RNA transcriptomes to identify base pair mismatches that did not represent genomic SNPs (Fig. 1B, C). To focus on high-confidence RNA editing events and exclude sequencing errors, DNA-RNA mismatches were filtered and excluded if the edited site was observed at low levels (<10% editing) or present in only a few neurons (<10 Ib or Is cells). Single cell DNA-RNA mismatches were also excluded if fewer than 10 total RNAseq reads covered the site, limiting editing calls for poorly expressed mRNAs within these neuronal populations. After filtering, 1637 high confidence RNA editing sites were identified across both motoneuron transcriptomes, of which 316 were canonical Adar-dependent A-to-I editing (Fig. 1D, Supplemental Tables 1, 2). A larger than expected set of C-to-T and G-to-A transversions were also observed (Fig. 1D, Supplemental Tables 3, 4), suggesting non-canonical editing also occurs in these neuronal populations. Although non-canonical editing has been described[64–67], the biological significance and molecular pathways mediating these edits are less clear. We largely focused on canonical A-to-I editing that is likely to have a greater impact on motoneuron function (Figs. 1-6), in contrast to non-canonical editing that appears less impactful based on the target sites identified (Supplemental Figs. 1, 2).

The 316 canonical edits identified were distributed across 210 genes and included 233 previously undescribed editing sites (Supplemental Table 2). Of these edits, 55% (175/316) occurred in mRNA coding sequences (CDS), while 36% (115/316) were in 3' UTR and 8% (26/316) in 5'UTR (Fig. 1E), consistent with prior editing distributions in *Drosophila*[47]. The editing rate within each region of the mRNA was normally distributed ($p < 0.05$, Kolmogorov-Smirnov test). Mean editing rate in the CDS (0.71) was significantly higher (ANOVA F statistic

= 20.171, degrees of freedom (df) = 2, Tukey $p < 7.8x10^{-10}$) than 3'UTR (0.59) and higher than 5'UTR editing (0.64), suggesting improved access or editing ability for Adar within the central coding region of transcripts compared to either end (Fig. 1F). For CDS edits, 58% (102/175) resulted in a missense amino acid substitution. Given edits that result in significant amino acid changes are more likely to alter protein function, we analyzed these edits in more detail. Missense changes were classified as significant if they altered the residue classification between (but not within) positive (R, K) or negative (D, E), hydrophobic (A, V, I, L, M, F, Y, W), polar (N, Q), potential phosphorylation sites (S, T), or structural resides (C, G, P, H). Based on these criteria, 59% (60/102) of missense edits resulted in significant alterations to the affected amino acid. The most common missense change was L>M, while the most common disruptive alteration was change of an existing residue into a glycine (S>G, E>G, R>G, and D>G, Fig. 1G). No canonical edit was identified that induced a premature stop codon. However, an edit in *Cnep1r2*, which encodes a serine/threonine phosphatase involved in nuclear pore formation and lipid metabolism[68], changed a stop codon into a tryptophan residue. The unedited transcript encodes a protein that is conserved with its mammalian homologs through the C-terminus, while the edited transcript creates a modified protein with an additional C-terminal 14 amino acids that could alter the protein's function. Ib motoneurons edited 54% of the total *Cnep1r2* mRNA, while Is neurons edited 28% of *Cnep1r2* mRNA.

Editing rules from single neuron analysis

Given this RNA editing analysis is based on single neurons with potentially distinct RNA editing patterns, we were interested in defining general rules for single cell editing compared to those observed using bulk RNAseq approaches. Early studies of editing rates for mammalian GluR2 AMPA receptors observed either a lack of editing or complete editing of *GluR2* mRNA depending on developmental stage, suggesting an all-or-none editing model. However, recent analyses of other sites suggest editing rates can be more variable[13,16,47,49]. To examine the editing profile across every editing site in individual Ib and Is neurons, the average fraction of edited reads in single cells was determined for each site (Fig. 1F). Editing rates spanned from the 10% threshold to 100% across both motoneuron populations. The average editing rate per site was 66% for both neuronal populations and was not significantly different (Fig. 1F, $p = 0.94$, Student's t-test, t statistic = 0.8, df=630). Consistent with prior editing studies in *Drosophila* adult CNS[16,23,24],

mRNAs encoding regulators of neuronal excitability and function were over-represented as editing targets in larval motoneuron transcriptomes (Fig. 2A). The largest number of edits (15 sites) occurred in the mRNA encoding Complexin (Cpx), a key regulator of synaptic vesicle fusion[69,70]. Other highly edited mRNAs included those encoding voltage-gated ion channels (Cac, Para, Shab, Sh, Slo), ligand-gated ion channels (nAChRalpha5, nAChRalpha6, nAChRalpha7, nAChRbeta1, Rdl) and regulators of synaptic transmission (EndoA, Syx1a, Rim, RBP, Vap33, Lap).

RNA editing events that induce critically important changes to a transcript would be predicted to be expressed in most cells. Although no edit site was detected in 100% of sampled neurons, often due to low read coverage at specific edit sites in any given cell, some edits were found in as many as 87% (175/206) of neurons. On average, an edited site was detected in ~19% (~40/206) of neurons (Fig. 2B). Edited sites observed in the largest fraction of sampled neurons are shown in Fig. 2C. Edits in the 5' and 3'UTR were more common in these cases, with edits in *ATPsynCF6* and *Syx1a* found in >80% of individual neurons. There was also a tendency for edit events to occur in proximity to other edits. Out of 315 sites, 53% had a nearby edit within 100 nucleotides and 26% had a nearby edit with 10 nucleotides (Fig. 2D), suggesting favorable Adar binding to some dsRNA regions increases editing rates at nearby adenosines[71]. Indeed, 12 edits with an average editing rate of 45% occurred in a stretch of 118 nucleotides in the 3'UTR of *Cpx* (3R:4301140-4301258). In summary, these data indicate RNA editing in larval motoneurons acts on a small number of target pre-mRNAs and ranges from low rates of editing to sites where the mRNA is fully edited.

Identification of editing sites that alter conserved amino acids

Amino acid changes that occur in conserved regions of a protein are more likely to have significant impact on function. We filtered the significant missense changes caused by editing and focused on those occurring in conserved residues or protein domains based on homology across other invertebrate or vertebrate species. 43 editing-induced significant missense changes were identified in conserved areas across several protein classes, including those regulating membrane excitability, synaptic transmission, and cell signaling (Table 1). 49% (21/43) of the edited residues altered amino acids that were conserved in vertebrates and invertebrates, while the remaining 51% (22/43) changed residues conserved across other insect homologs. Notably, many of the edits

occurred within annotated protein domains. Given these edits alter conserved amino acids and are likely to have a larger impact on larval motoneuron function, they were examined in more detail.

Multiple subunits of the nicotinic acetylcholine receptor (nAChR) family, which function as ligand-gated cation channels mediating fast excitatory neurotransmission, were found to undergo editing. One edit in nAChRalpha5 converts a threonine to alanine (T791A) in the 4th transmembrane domain and is edited at very high levels (Ib: 99%, Is: 96%, Fig. 3A), suggesting the edited version represents the majority of nAChRalpha5 protein in motoneurons. Edits in nAChRalpha6 (Fig. 3B) and nAChRbeta1 (Fig. 3C) altered conserved residues in the extracellular ligand-binding domains of the proteins. Editing also occurred in several proteins regulating neuronal excitability, including E-to-G and Y-to-C edits in the ATPalpha sodium pump (Fig. 3D), a highly edited S-to-G site (Ib: 86%, Is: 91%) in the 9th transmembrane segment of the voltage-gated calcium channel Cacophony (Fig. 3E), and multiple edits in the ion transport domain of other voltage-gated ion channels, including Shab, Sh, Slo and Para (Fig. 3F).

Beyond neuronal excitability, mRNAs encoding proteins regulating the synaptic vesicle cycle were also editing targets (Table 1). Three edit sites within the C-terminal domain of the Cpx7A splice isoform were identified and previously described[27]. Editing of adjacent adenosines encoding the N130 amino acid produce N130S, N130G or N130D variants that alter Cpx's ability to regulate synaptic vesicle fusion[27]. Editing was also observed in a key regulator of endocytosis, Endophilin A (EndoA), resulting in a change from a positively charged K to a negatively charged E residue at amino acid 140 within the F-BAR lipid-binding domain. Given the K residue is conserved in all Endophilin homologs, one would predict this charge substitution alters EndoA function in endocytosis within motoneurons. Editing of another synaptic vesicle endocytosis regulator, the Clathrin AP180 adaptor homolog Lap, occurred at high rates (Ib: 88%, Is: 95%) and resulted in a T-to-A change in a conserved residue. Edits were also identified in the AZ proteins Rim and RBP that altered C-terminal residues conserved in other insect homologs. Similarly, an edit in the VhaAC45RP subunit of the synaptic vesicle proton pump resulted in neutralization of a negatively charged E residue conserved in other insect homologs.

Within the group of edits predicted to significantly impact protein function, 67% (29/43) were previously annotated on FlyBase as editing sites, while 33% (14/43) were not previously described. Newly identified sites could be enriched targets for 3rd instar larval motoneurons or missed in prior work. Among the new edits was a missense D-to-G change in Bsk (Fig. 3G), a

conserved serine/threonine protein kinase central to the stress-induced c-Jun N-terminal kinase (JNK) pathway. The edited D residue is universally conserved in JNK kinase homologs and resides within the core of the kinase domain. Editing from D to G occurs at moderate levels (Ib: 34%, Is: 30%) and is predicted to be disruptive to the protein's function. Another novel editing site was identified in the spliceosomal protein Beag (Fig. 3H). Beag forms a complex with Smu1 and additional alternative splicing proteins and is required for larval synapse development and function[72]. The edited serine residue is conserved across insect species and is edited at high rates within motoneurons (Ib: 72%, Is: 57%). The S-to-G substitution occurs in the RED-like protein C-terminal domain, a region involved in nuclear localization and binding to other nuclear-localized proteins[73]. A third newly identified edit site results in an E-to-G substitution in the highly conserved endoribonuclease RNase Z (Fig. 3I) involved in tRNA processing[74]. The E744 residue is universally conserved in invertebrate and vertebrate homologs and localizes downstream of its metallo-beta-lactamase C-terminal domain. This site is edited at high levels in larval motoneurons (Ib: 90%, Is: 100%) and is predicted to significantly impact the protein's function. An additional previously undescribed edit site occurred in *Opa1*, encoding a dynamin-related GTPase that mediates mitochondrial fusion[75,76]. This site was robustly edited (Ib: 80%, Is: 74%) and represented the only site identified that "re-coded" a non-conserved amino acid (N) into a residue (E) that was universally conserved in all other Opa1 homologs. These data indicate RNA editing alters highly conserved residues across several proteins, including those involved in membrane excitability and synaptic transmission that are likely to impact the development and function of larval motoneurons.

Characterization of highly edited transcripts and editing stochasticity

We next examined sites with a very high editing rate that also induced missense amino acid substitutions to identify edits that may cause larger functional impacts on motoneurons similar to mammalian AMPA receptor editing. 27 sites in 18 genes were found to be edited at >90% levels in Ib or Is neurons that underwent editing at the location (Supplemental Table 5). 85% (23/27) of these sites were previously annotated on FlyBase, consistent with these targets being more commonly identified given their high editing rate. Highly edited sites were overrepresented in genes regulating membrane excitability and synaptic function. 10 sites in 9 genes displayed 100% editing in at least one of the two neuronal populations, including: (1) *quiver*, a trafficking regulator

of K^+ and nACH receptors; (2, 3) *nAChRalpha5* and *nAChRalpha6,* subunits of the nicotinic acetylcholine receptor; (4) *Prosap*, the *Drosophila* SHANK synaptic scaffolding homolog; (5) *Rdl*, a GABA receptor; (6) *Nckx30C*, a Na^+/K^+-dependent Ca^{2+} exchanger; (7) *Shab*, a delayed rectifier K^+ channel; (8) *Ythdc1*, a regulator of alternative splicing; and (9) *RNaseZ*, a pre-tRNA endoribonuclease. Although these sites were highly edited, most sites showed more variable patterns of editing, with some neurons editing the site at high levels while others had lower rates or no editing. Despite the observation that average *Adar* mRNA levels were not significantly different between Ib and Is neurons (Fig. 4A, $p = 0.55$, adjusted p-value from RNA sequencing Wald statistic[61]), editing differences could be related to Adar expression within individual motoneurons. Similar to prior studies[13–15,17], *Adar* mRNA expression level at the resolution of single cells did not correlate with overall editing rates (Fig. 4B). Indeed, neurons with low or high *Adar* transcript levels were able to edit specific sites up to 100%. However, we noticed that edit sites in abundantly expressed mRNAs (expression level in the top 30% as noted by red dots in Fig. 4B) generally had lower editing rates. Given 4000-fold differences in gene expression can occur across transcripts within larval motoneurons[61], we hypothesized that abundant transcripts might result in lower editing if Adar activity becomes rate-limiting. Indeed, mRNA expression level was inversely correlated to the fraction of reads edited at individual sites for both Ib and Is subtypes (Ib: Pearson's $r = -0.59$, $r^2 = 0.35$; Is: $r = -0.58$, $r^2 = 0.34$, Fig. 4C). We conclude that editing levels are not directly limited by Adar expression but rather by target gene expression, suggesting Adar can become rate-limiting when high levels of an editable pre-mRNA transcript are present.

Although *Adar* mRNA levels did not correlate with editing rate, it is possible the expression of other RNA binding proteins or editing factors impact the rate of editing. If so, one would expect certain neurons to display higher overall editing rates than others. To examine this possibility, editing rate for every target site was plotted for each individual Ib and Is motoneuron (Fig. 4D). Neurons from both populations displayed a range of average editing rates across all target sites that varied from ~30% to >80% (Fig. 4D). Although it is unclear what drives these differences in editing rate for neurons of the same cell type, future analysis of DEGs between "low editors" and "high editors" might identify candidate proteins that impact editing across an otherwise homogenous neuronal population. Another possibility for differential editing is that cells with the highest editing rate edit fewer transcripts overall. Consistent with this model, the mean fraction of reads edited versus the number of edits across individual neurons displayed a negative correlation

(Ib: Pearson's r = -0.33, r^2 = 0.11; Is: r = -0.50, r^2 = 0.25, Fig. 4E). We hypothesized that an edit found in most cells would potentially have a high editing rate. However, a negative correlation was observed, suggesting the more cells an edit was found in, the lower the mean editing rate (Fig. 4F). Beyond variability in editing rate, some mRNAs displayed a highly stochastic nature of editing where many cells expressed a mixture of edited and unedited mRNA, whereas others had all or none editing for that same target site. Several representative regions showing stochastic editing rates are shown for three such edits in *Cpx* (Fig. 4G). In summary, editing rates for most target sites is variable at the level of single neurons and individual edited adenosine residues, with only a small number of sites undergoing complete editing.

Comparison of RNA editing between Ib and Is motoneuron populations

Given structural and functional differences between tonic Ib and phasic Is motoneurons, we hypothesized unique RNA editing targets may help establish their distinct features. However, the overall landscape of RNA editing across Ib and Is neurons was similar at the level of edit site location (5'UTR, CDS, 3'UTR) and editing rate (Fig. 1F). In addition, the number of edit sites and fraction of reads edited per cell showed similar profiles (Fig. 5A). A comparison of editing rate at individual sites indicated most were edited to the same level between Ib and Is neurons (Pearson's r = 0.73, r^2 = 0.53, Fig. 5B). The fraction of Ib and Is motoneurons that expressed individual edits was also correlated (Pearson's r = 0.83, r^2 = 0.69), although several edits were only detected in one of the two cell types (red and blue dots in Fig. 5C). Though editing rules were generally similar between the two populations, several differences emerged. The lower tail of the distribution for the fraction of edited reads displayed a sharper drop across Ib cells (Fig. 4D), indicating a subset of these neurons have distinctly lower editing rates than observed in Is neurons. Similarly, the upper tail of the distribution revealed a subset of Is neurons with higher editing rates than observed within the Ib population (Fig. 4D).

To identify sites with significantly different editing rates between subtypes, differentially expressed mRNAs were removed from the analysis. Following DEG filtering, 26 RNA edit sites across 22 genes were identified that displayed statistically significant editing differences (Fig. 5D, E, Supplemental Table 6). Although 3'UTR edits comprised only 36% of all editing sites (Fig. 1B), 46% (12/26) of differentially edited sites between Ib and Is neurons were in 3'UTRs. Given 3'UTR editing can modify microRNA binding sites or protein translation rates, it is interesting to

consider if post-transcriptional regulation through RNA editing in this region differentially impacts protein production. Of particular interest are two 3'UTR sites in *complexin* (3R:4301150 and 3R:4301158) that are edited at greater rates in Is neurons, which are known to express lower Cpx protein levels at synapses[77]. Several targets were also edited in only one of the two cell populations. Ntf-2, a regulator of nuclear import, had a 3'UTR edit that was only observed in Is neurons (edit rate: 0% in Ib, 92% in Is). In contrast, Fipi (NCAM2 homolog regulating neuronal structure, edit rate: 54% in Ib, 0% in Is), CG31650 (Reticulocalbin 2 homolog involved in ER Ca^{2+} homeostasis, edit rate: 70% in Ib, 0% in Is) and CG4502 (E2 ubiquitin-conjugating enzyme, edit rate: 73% in Ib, 0% in Is) were only edited in Ib neurons. Like Ntf-2, the Fipi edit localizes to the 3'UTR. The CG4502 Ib-only edit is unlikely to have a functional impact as it causes a silent CDS change, while the CG31650 Ib-only edit causes a H39R amino acid substitution within a non-conserved part of the protein that lies outside of its five Ca^{2+}-binding EF hand domains. We conclude that differential editing between Ib and Is neurons that alters amino acid identity is rare and unlikely to play a major role in the morphological and functional diversity between these neuronal populations. Differential editing within the 3'UTR of several genes could impact expression of their encoded proteins, but neuronal subtype diversity of Ib and Is cells appears to be driven mostly by their unique DEGs rather than differential RNA editing.

Larval muscles have fewer editing targets and reduced editing rate per site compared to motoneurons

To compare the editing landscape of motoneurons with a non-neuronal cell type, Patch-seq data generated from larval abdominal muscles 1 and 4[61], postsynaptic targets for Ib and Is motoneurons (Fig. 1C), was analyzed using the same pipeline as described above. Like other skeletal muscles, *Drosophila* bodywall muscles are generated from fusion of individual myocytes, forming polynuclear cells containing ~8-20 nuclei that share a common cytoplasm[78]. As such, Patch-seq from larval muscles is likely to sample a larger population of editing possibilities compared to single nuclei motoneurons. Despite being polynucleated, only 37 canonical editing sites were detected in at least 10 muscle samples that had >10% editing rate (Supplemental Tables 1, 2, and 7, Fig. 6A). Seven of these sites were uniquely edited in muscles and the remaining 30 were also present in Ib or Is motoneurons (Fig. 6A). Muscle cells displayed similar or lower editing rates than Ib or Is neurons at shared edit sites (Fig. 6B, Supplemental Table 2). Muscle-specific

editing sites (Supplemental Table 7) were enriched for highly expressed muscle genes, including *Act5C* (Actin homolog), *wupA* (Troponin 1 homolog), *TpnC47D* (Troponin C homolog) and *mthl3* (Secretin-like GPCR). Like motoneurons, editing rate in muscles was variable for specific target sites, ranging from 18% at the lower end to 75% edited (Supplemental Table 7). Compared to an average editing rate per site of 66% for motoneuron targets, the average editing rate for muscle-only targets was only 34%. In addition, *Adar* mRNA levels were 2-fold lower in muscles (0.91 TPM) compared to motoneurons (1.89 TPM, $p = 0.0019$, Student's t-test, t statistic = -3.14, df = 247)[61]. These data indicate larval motoneurons have more editing sites and higher editing rates than their postsynaptic muscle targets, consistent with RNA editing having a greater impact on neuronal function.

Noncanonical RNA editing is observed in larval motoneurons but results in fewer significant amino acid changes

Although canonical A-to-I Adar-dependent deamination is well-known, other forms of mRNA editing have been described and are emerging in importance due to their application in targeted genome editing[79–81]. By comparing motoneuron and muscle transcriptomes to parental genome sequences, we identified non-canonical ribonucleoside substitutions (non-A-to-I) across several mRNAs (Fig. 1D, Supplemental Tables 3, 4). A similar percent of edits occurred in the CDS for canonical (55%) and non-canonical (48%) editing (Supplemental Fig. 1A, B). However, the ratio of silent changes was much higher for non-canonical edits (70% versus 42%, Supplemental Fig. 1C). Although fewer of these edits resulted in an amino acid change, they generated a distinct pattern of substitutions compared to Adar-dependent editing (Supplemental Fig. 1D). Unlike canonical editing, non-canonical edit sites were not enriched for neuron-specific genes (Supplemental Table 4, Supplemental Fig. 1E). However, the overall fraction of cells displaying non-canonical RNA edits (Supplemental Fig. 1F) and the likelihood of edits to cluster near each other (Supplemental Fig. 1G) were similar to Adar-dependent editing.

Other features of non-canonical editing also mirrored Adar-dependent editing, including evidence for a rate-limiting editing machinery for abundantly edited transcripts (Supplemental Fig. 2A) and a reduced number of overall edits for cells with a high editing rate (Supplemental Fig. 2B). Non-canonical editing also exhibited variability in editing rate per site across individual cells for both Ib and Is subtypes, with some neurons displaying higher or lower rates (Supplemental Fig.

2C). Overall, Ib and Is neurons showed similar numbers of edited sites (Supplemental Fig. 2D), editing rate per individual site (Supplemental Fig. 2E), and the fraction of cells containing a specific non-canonical edit (Supplemental Fig. 2F). Only a few non-canonical edits were identified that altered conserved residues in key neuronal proteins (Supplemental Table 4), suggesting a limited impact for these edits on motoneuron function. Of the non-canonical edits, an amino acid substitution in the Arc1 protein (P124L) was induced by a C-to-T edit that altered a P residue conserved in other insect Arc homologs. Given the role of Arc in synaptic plasticity in *Drosophila*[82], it will be interesting to examine if this change alters Arc capsid assembly or function. Another non-canonical edit of potential significance was identified in muscles, where a C-to-T edit caused a P-to-S substitution in a highly conserved residue in the C-terminal LDLR domain of Nidogen (Ndg), a core component of the basement membrane. The most significant change observed was in the mRNA encoding CG3760, a homolog of mammalian CDV3 (carnitine deficiency-associated protein 3). A G-to-A edit in CG3760 induced a premature stop codon at amino acid 152 (W152*), truncating the C-terminal 119 amino acids of the protein. Although CG3760 is widely expressed in multiple tissue types, its function is unknown. A mutation in CG3760 was identified as a partial suppressor for a temperature-sensitive paralytic mutation in the t-SNARE Syntaxin 1[83,84], indicating a possible role in synaptic function. Ib motoneurons edited 56% and Is neurons edited 45% of CG3760 mRNA, suggesting this non-canonical edit may play a proteostasis role by reducing CG3760 protein abundance in motoneurons. Given the lack of neuronally-enriched target sites and a larger propensity for generating silent coding changes, these data suggest non-canonical editing does not play as significant a biological role in generating functional protein diversity compared to canonical A-to-I editing within larval motoneurons.

Discussion

Multiple types of ribonucleoside modifications occur across mRNAs, tRNAs, rRNAs and ncRNAs[67]. RNA editing modifies single nucleotides in mRNA transcripts in a cell-type-specific manner and is one of the more widely observed RNA modifications across metazoans. In this study, we characterized the RNA editing landscape of individual *Drosophila* 3rd instar larval motoneuron populations using Patch-seq RNA extraction to define rules for single cell editing and identify the most relevant editing targets. Tonic-like Ib and phasic-like Is motoneurons form well-studied glutamatergic synapses with cell-type-specific electrophysiological and morphological features, providing a model system to investigate how RNA editing contributes to their morphology and function, as well as any role in cell-type-specific diversity. Most A-to-I edits identified in our study occurred within mRNA coding regions, with many of these changes predicted to cause significant alterations to protein function. As observed in prior studies[9,16,23–25], mRNAs encoding ion channels and synaptic proteins represented some of the most highly edited targets, suggesting editing of these gene classes are likely to fine tune membrane excitability and synaptic output in larval motoneurons. The overall RNA editing landscape was similar across Ib and Is populations, indicating differences in editing targets or editing rate is unlikely to be a major driver of cell-type diversity for these neuronal subtypes.

Using single cell sequencing from stereotyped and identified single Ib and Is motoneurons, this analysis revealed a wide variation in average RNA editing levels for specific sites and across individual cells. Indeed, many sites underwent highly stochastic editing when compared across the neuronal population. For example, some neurons displayed ~100% editing at certain sites, while others displayed no editing for the same target. Such dramatic differences in editing rate at specific target sites is likely to contribute to the heterogenous features observed within the same neuronal population. For cases where editing variability is restricted to a narrower range, neurons would be predicted to express a population of both edited and unedited proteins. What drives the variability in RNA editing across individual motoneurons is unclear. Given Adar is an enzyme, its affinity for specific dsRNA structures plays a role in establishing editing levels for any specific pre-mRNA target site. Although *Adar* mRNA level in individual neurons was not correlated with editing rate, the expression level of the target mRNA undergoing editing was a major factor. Indeed, mRNA expression level was anti-correlated with editing percent, suggesting *Drosophila* Adar activity becomes rate-limiting for abundant pre-mRNAs as proposed in mammals[7]. Beyond mRNA

expression level, variable expression of other trans-acting factors that regulate Adar function or pre-mRNA accessibility could modulate editing rate or target site selection across individual neurons as previously hypothesized[85].

Although this study defines the RNA editing landscape for *Drosophila* larval motoneurons, future experiments will be required to elucidate how specific RNA editing events regulate target gene expression or protein function. Of particular interest will be edits occurring at high levels, such as the 3'UTR edit in *ATPsynCF6* and 5'UTR edits in *Syx1A*, as these may represent edits required for normal transcript localization, expression, or function. For editing events that lead to amino acid change, these substitutions could in principle improve, disrupt, or modify protein function. Only one edit event "re-coded" an amino acid from a non-conserved residue into a residue conserved in orthologous proteins (a N to D edit in the mitochondrial fusion protein Opa1), suggesting most coding edits with a functional effect are likely to diversify or disrupt protein activity as previously suggested based on comparative genomics[86,87]. The evolutionarily advantage, if any, that RNA editing has in modifying protein function is still unclear. One hypothesis is that RNA editing plays similar roles to alternative splicing. For example, changes in the ratio of Unc13A and Unc13B splice isoforms during *Drosophila* active zone development regulate the probability of synaptic vesicle release by altering the position of docked synaptic vesicles near Ca^{2+} channels[88,89]. In a similar manner, ratiometric pools of edited versus unedited proteins could provide a mechanism to fine-tune specific neuronal features, particularly for proteins whose abundance is rate-limiting or that act within multimeric complexes. Such a mechanism has been observed for distinct Cpx edit variants[27], where individual Cpx proteins are required to clamp multiple assembling SNAREpins during synaptic vesicle priming. In addition, functional properties of the Shaker voltage-gated K^+ channel are shaped by the combination of individual edits across 4 distinct sites[85].

Although canonical and non-canonical (non-A-to-I) editing was observed in larval motoneurons, Adar-dependent editing resulted in far more edits to neuronal-specific genes predicted to impact protein function. The majority of non-canonical CDS edits caused silent changes, suggesting evolutionary selection against this mechanism as a pathway for generating protein diversity. One non-canonical C-to-U coding edit of interest caused a P124L amino acid change in the activity-regulated *Arc1* mRNA that encodes a retroviral-like Gag protein involved in synaptic plasticity[90]. Approximately 50% of total *Arc1* mRNA was edited at this site in both Ib

and Is neurons. Given *Drosophila* Arc1 assembles into higher order viral-like capsids similar to mammalian Arc proteins[91], it will be interesting to determine if and how this amino acid change might alter capsid formation or structure. In terms of the underlying editing machinery, the mammalian APOBEC cytosine deaminases generate C-to-U edits in target mRNAs like *apoB*[92]. The *Drosophila* genome encodes three predicted cytosine deaminases (CG8349, CG8353 and CG8360), though their role in editing has not been studied. Other forms of editing, including G-to-A and U-to-C, have also been described in mammals[93,94], though the machinery that mediates these events is unclear. The most significant remaining non-canonical edit we observed occurred in the mRNA encoding CG3760, a homolog of mammalian CDV3. A G-to-A edit in this poorly characterized gene resulted in a premature stop codon that truncated the last ~40% of the protein. Given ~50% of CG3760 mRNA contained this edit, we hypothesize this may represent a case of editing-regulated proteostasis if the truncated protein undergoes degradation. Outside of these cases, it seems unlikely that non-canonical editing plays a major role in regulating larval motoneuron function compared to Adar-dependent editing.

Materials and Methods

Single cell RNA sequencing

RNA sequencing data from 105 MN1-Ib and 101 MNISN-Is motoneurons (GEO accession #GSE222976)[61] was used for editing analysis. 10XUAS-mCD8-GFP (RRID:BDSC_32185) was expressed using either a Ib-specific (RRID: BDSC_40701) or Is-specific (RRID: BDSC_49227) Gal4 driver. The nucleus and surrounding cytoplasm of GFP+ motoneurons in 3rd instar larvae were extracted using a patch pipet and immediately frozen on dry ice. cDNA was generated, purified, dual indexed, and run on an Illumina NextSeq500 (paired-end 75 nt reads) sequencer as described[61].

Genome sequencing

High purity genomic DNA from parental Ib-Gal4, Is-Gal4, and 10XUAS-mCD8-GFP lines was collected and sequenced. Flies were grown at 25°C. 10 adult male flies from each genotype were collected under CO_2 anesthetization into a 1.5mL centrifuge tube and immediately frozen in liquid nitrogen. 120 µL of grinding buffer (0.2 M sucrose, 0.1 M Tris pH 9.2, 50 mM EDTA, 0.5% SDS) was added and a VWR pellet mixer (VWR, cat# 47747-370) was used to homogenize the flies for one minute. Samples were vortexed for 10 seconds and placed on ice for 15 minutes. 500 µL of Phenol:Chloroform:Isoamyl Alcohol (Millipore-Sigma, SKU# 6805-100ML, Omnipur 25:24:1 and TE Buffered Saturated pH 6.7/8.0) was added and vortexed for 30 seconds. Samples were centrifuged at 16,100 relative centrifugal force (RCF) for 5 minutes to pellet debris and separate protein to the interphase and DNA in the upper phase. The DNA-containing upper phase was pipetted into 1 mL of 100% ethanol in a new 1.5 mL tube and vortexed briefly to mix. After incubation overnight at 4°C, samples were centrifuged at 16,100 RCF for 10 minutes to pellet DNA. The pellet was washed in 70% ethanol by pipetting, centrifuged at 16,100 RCF for 10 minutes, and the pellet air-dried for 30 minutes. 50 µL of DNAse-free ultrapure water was added to each sample and incubated at 37°C for 15 minutes before resuspension. DNA samples were prepared as libraries for sequencing using the Nextera DNA Flex (Illumina) kit and sequenced on an Illumina NextSeq500.

RNA edit detection and parental DNA variation calling

Paired-end fastq files were mapped to *Drosophila_melanogaster*.BDGP6.92 reference using BWA. Sequencing reads with mapping quality score less than 5 were removed from downstream analyses using Samtools. PCR duplicates were removed using GATK MarkDuplicatesSpark. The variations were first called using Samtools mpileup, and the high-quality SNPs (depth>=8 and quality score >=20) and indels were selected as the database of known polymorphic sites for GATK base quality recalibration. Base quality recalibration was accomplished using GATK BaseRecalibrator and ApplyBQSR. Variations were then called by GATK HaplotypeCaller with VCF outputs. Variations were subset to exonic regions only. Only SNPs were kept for downstream filtering. Since genes localize to both DNA strands while RNA sequencing reads are only aligned to the positive strand, A-to-G editing in minus strand genes appear as T-to-C. To facilitate data analysis, edits in minus strand genes are listed as their reverse complement in the text.

Filtering RNA variations against parental DNA SNPs

SNPs in RNA samples were excluded if they existed in any of the three parental DNA samples as determined by GATK Haplotypecaller and Samtools mpileup based on genomic location and genotype. To prevent mapping complication of nearby indels, RNA SNPs with indels within 10 bp were filtered out. The remaining RNA SNPs were selected as candidate RNA editing sites for further validation.

Filtering of candidate RNA edits

A custom MATLAB code was used to further analyze and filter variant call output from Samtools and GATK. Potential edits were removed if (1) there were ≤ 10 RNA sequencing reads covering this genomic location, (2) the GATK Phred-scaled probability (QUAL score) of a polymorphism was ≤ 20, (3) the cell-specific edit site had ≤ 10% editing rate, (4) the edit was found in fewer than 10 Ib or Is cells, or (5) less than 96% of the sequenced genomic DNA nucleotide at this site failed to match the reference genome (a genomic SNP). Remaining edits were processed to categorize where in the gene the edit occurred. In rare occasions, edits occurred in overlapping genes. In these cases, only edits occurring within exons were kept and listed as an edit in each gene if more than one gene had an exon at this location. Manual inspection revealed many non-canonical edits/SNPs clustered near the beginning of the 5'UTR (where sequencing errors were more common), so edits

< 20 nucleotides from the 5'UTR start site were excluded. The remaining high confidence edit sites were analyzed to provide summary statistics, including average editing rate across Ib and Is neurons. Gene boundaries for CDS, 5'UTR and 3'UTR, previously annotated A-to-I editing events, gene descriptions, Pfam locations, and other genome-related information were downloaded from FlyBase on Sept 15 2023.

Software and code

Software versions were as follows: Star (2.5.3a), BWA (0.7.12), Samtools (1.10), GATK (4.1.2.0), MATLAB (2022b). The full MATLAB code with instructions for RNA editing analysis is downloadable as a ZIP file from Supplemental Material.

RNA editing conservation analysis

Canonical RNA edits that led to a missense change in the translated amino acid were analyzed to determine if the RNA editing site changed an amino acid that was conserved across species. NCBI BLAST was used to locate the relevant amino acid in polypeptide strings of other insects or mammals and compared to the *Drosophila melanogaster* reference genome. Sites were considered conserved if the unedited amino acid at this location was identical between *Drosophila melanogaster* and other species.

Statistical analysis

For comparisons between two groups, statistical significance was determined using an unpaired, two-tailed, two-sample Student's t-test. For comparisons between three or more groups, statistical significance was determined using a one-way ANOVA followed by the Tukey-Kramer post-hoc multiple comparisons test. Figures depict the mean of each distribution and individual data points, and asterisks denote p values of: *, $p \leq 0.05$; **, $p \leq 0.01$; ***, $p \leq 0.001$; and ****, $p \leq 0.0001$. Normalcy of data distribution was determined using the one-sample Kolmogorov-Smirnov test. The correlation coefficient (r) between two sets of data was determined using the Pearson correlation method.

Data Availability

The authors declare the source data supporting this study are available within the paper, supplementary material and indicated repositories. RNA sequencing data is available at the GEO data repository (accession #GSE222976). DNA sequencing data for parental genotypes is available at the NCBI BioSample Database (accession #PRJNA1112347). MATLAB codes are provided in Supplemental Material.

Acknowledgements

This work was supported by NIH grants MH104536 and NS117588 to J.T.L. AB.C. was supported in part by NIH pre-doctoral training grant F31NS118948. We thank the Bloomington *Drosophila* Stock Center (NIH P40OD018537) for providing *Drosophila* strains, Duanduan Ma and Charlie Whittaker for help with genomic and editing analysis, and members of the Littleton lab for helpful discussions and comments on the project and manuscript.

Competing interests

The authors declare no competing interests.

Author contributions

Conceptualization, A.B.C and J.T.L.; methodology, A.B.C. and S.K.J,; investigation, A.B.C. and J.T.L.; funding acquisition, J.T.L.; supervision, J.T.L.; writing—original draft, A.B.C. and J.T.L.; writing—review & editing, A.B.C., S.K.J. and J.T.L.

References

1. Rieder, L. E. & Reenan, R. A. The intricate relationship between RNA structure, editing, and splicing. *Semin. Cell Dev. Biol.* **23**, 281–288 (2012).

2. Shevchenko, G. & Morris, K. V. All I's on the RADAR: role of ADAR in gene regulation. *FEBS Lett.* **592**, 2860–2873 (2018).

3. Nishikura, K. Functions and regulation of RNA editing by ADAR deaminases. *Annu. Rev. Biochem.* **79**, 321–349 (2010).

4. Berkovits, B. D. & Mayr, C. Alternative 3' UTRs act as scaffolds to regulate membrane protein localization. *Nature* **522**, 363–367 (2015).

5. Borchert, G. M. *et al.* Adenosine deamination in human transcripts generates novel microRNA binding sites. *Hum. Mol. Genet.* **18**, 4801–4807 (2009).

6. Lev-Maor, G. *et al.* RNA-editing-mediated exon evolution. *Genome Biol.* **8**, R29 (2007).

7. Lopdell, T. J. *et al.* Widespread cis-regulation of RNA editing in a large mammal. *RNA* **25**, 319–335 (2019).

8. Nakano, M., Fukami, T., Gotoh, S. & Nakajima, M. A-to-I RNA Editing Up-regulates Human Dihydrofolate Reductase in Breast Cancer. *J. Biol. Chem.* **292**, 4873–4884 (2017).

9. Rueter, S. M., Dawson, T. R. & Emeson, R. B. Regulation of alternative splicing by RNA editing. *Nature* **399**, 75–80 (1999).

10. Stellos, K. *et al.* Adenosine-to-inosine RNA editing controls cathepsin S expression in atherosclerosis by enabling HuR-mediated post-transcriptional regulation. *Nat. Med.* **22**, 1140–1150 (2016).

11. Yuan, J. *et al.* Biological roles of A-to-I editing: implications in innate immunity, cell death, and cancer immunotherapy. *J. Exp. Clin. Cancer Res.* **42**, 149 (2023).

12. Mazloomian, A. & Meyer, I. M. Genome-wide identification and characterization of tissue-specific RNA editing events in D. melanogaster and their potential role in regulating alternative splicing. *RNA Biol.* **12**, 1391–1401 (2015).

13. Graveley, B. R. *et al.* The developmental transcriptome of Drosophila melanogaster. *Nature* **471**, 473–479 (2011).

14. Lundin, E. *et al.* Spatiotemporal mapping of RNA editing in the developing mouse brain using in situ sequencing reveals regional and cell-type-specific regulation. *BMC Biol.* **18**, 6 (2020).

15. Picardi, E., Horner, D. S. & Pesole, G. Single-cell transcriptomics reveals specific RNA editing signatures in the human brain. *RNA* **23**, 860–865 (2017).

16. Sapiro, A. L. *et al.* Illuminating spatial A-to-I RNA editing signatures within the Drosophila brain. *Proc Natl Acad Sci USA* **116**, 2318–2327 (2019).

17. Wahlstedt, H., Daniel, C., Ensterö, M. & Ohman, M. Large-scale mRNA sequencing determines global regulation of RNA editing during brain development. *Genome Res.* **19**, 978–986 (2009).

18. Birk, M. A. *et al.* Temperature-dependent RNA editing in octopus extensively recodes the neural proteome. *Cell* **186**, 2544-2555.e13 (2023).

19. Kliuchnikova, A. A. *et al.* Proteome-Wide Analysis of ADAR-Mediated Messenger RNA Editing during Fruit Fly Ontogeny. *J. Proteome Res.* **19**, 4046–4060 (2020).

20. Buchumenski, I. *et al.* Dynamic hyper-editing underlies temperature adaptation in Drosophila. *PLoS Genet.* **13**, e1006931 (2017).

21. Ma, E., Tucker, M. C., Chen, Q. & Haddad, G. G. Developmental expression and enzymatic activity of pre-mRNA deaminase in Drosophila melanogaster. *Brain Res. Mol. Brain Res.* **102**, 100–104 (2002).

22. Alon, S. *et al.* The majority of transcripts in the squid nervous system are extensively recoded by A-to-I RNA editing. *eLife* **4**, (2015).

23. Hoopengardner, B., Bhalla, T., Staber, C. & Reenan, R. Nervous system targets of RNA editing identified by comparative genomics. *Science* **301**, 832–836 (2003).

24. Palladino, M. J., Keegan, L. P., O'Connell, M. A. & Reenan, R. A. A-to-I pre-mRNA editing in Drosophila is primarily involved in adult nervous system function and integrity. *Cell* **102**, 437–449 (2000).

25. Jepson, J. E. C. & Reenan, R. A. Adenosine-to-inosine genetic recoding is required in the adult stage nervous system for coordinated behavior in Drosophila. *J. Biol. Chem.* **284**, 31391–31400 (2009).

26. Brusa, R. *et al.* Early-onset epilepsy and postnatal lethality associated with an editing-deficient GluR-B allele in mice. *Science* **270**, 1677–1680 (1995).

27. Brija, E. A., Guan, Z., Jetti, S. K. & Littleton, J. T. Stochastic RNA editing of the Complexin C-terminus within single neurons regulates neurotransmitter release. *Cell Rep.* **42**, 113152 (2023).

28. Eisenberg, E. & Levanon, E. Y. A-to-I RNA editing - immune protector and transcriptome diversifier. *Nat. Rev. Genet.* **19**, 473–490 (2018).

29. Athanasiadis, A., Rich, A. & Maas, S. Widespread A-to-I RNA editing of Alu-containing mRNAs in the human transcriptome. *PLoS Biol.* **2**, e391 (2004).

30. Bazak, L. *et al.* A-to-I RNA editing occurs at over a hundred million genomic sites, located in a majority of human genes. *Genome Res.* **24**, 365–376 (2014).

31. Levanon, E. Y. *et al.* Systematic identification of abundant A-to-I editing sites in the human transcriptome. *Nat. Biotechnol.* **22**, 1001–1005 (2004).

32. Dracheva, S. *et al.* Increased serotonin 2C receptor mRNA editing: a possible risk factor for suicide. *Mol. Psychiatry* **13**, 1001–1010 (2008).

33. Ferrick-Kiddie, E. A., Rosenthal, J. J. C., Ayers, G. D. & Emeson, R. B. Mutations underlying Episodic Ataxia type-1 antagonize Kv1.1 RNA editing. *Sci. Rep.* **7**, 41095 (2017).

34. Yang, Y., Okada, S. & Sakurai, M. Adenosine-to-inosine RNA editing in neurological development and disease. *RNA Biol.* **18**, 999–1013 (2021).

35. Tassinari, V. *et al.* Contribution of A-to-I RNA editing, M6A RNA Methylation, and Alternative Splicing to physiological brain aging and neurodegenerative diseases. *Mech. Ageing Dev.* **212**, 111807 (2023).

36. Hosaka, T., Tsuji, H. & Kwak, S. Roles of aging, circular rnas, and RNA editing in the pathogenesis of amyotrophic lateral sclerosis: potential biomarkers and therapeutic targets. *Cells* **12**, (2023).

37. Sommer, B., Köhler, M., Sprengel, R. & Seeburg, P. H. RNA editing in brain controls a determinant of ion flow in glutamate-gated channels. *Cell* **67**, 11–19 (1991).

38. Köhler, M., Burnashev, N., Sakmann, B. & Seeburg, P. H. Determinants of Ca2+ permeability in both TM1 and TM2 of high affinity kainate receptor channels: diversity by RNA editing. *Neuron* **10**, 491–500 (1993).

39. Higuchi, M. *et al.* Point mutation in an AMPA receptor gene rescues lethality in mice deficient in the RNA-editing enzyme ADAR2. *Nature* **406**, 78–81 (2000).

40. Peng, P. L. *et al.* ADAR2-dependent RNA editing of AMPA receptor subunit GluR2 determines vulnerability of neurons in forebrain ischemia. *Neuron* **49**, 719–733 (2006).

41. Yamashita, T. & Kwak, S. The molecular link between inefficient GluA2 Q/R site-RNA editing and TDP-43 pathology in motor neurons of sporadic amyotrophic lateral sclerosis patients. *Brain Res.* **1584**, 28–38 (2014).

42. Takuma, H., Kwak, S., Yoshizawa, T. & Kanazawa, I. Reduction of GluR2 RNA editing, a molecular change that increases calcium influx through AMPA receptors, selective in

the spinal ventral gray of patients with amyotrophic lateral sclerosis. *Ann. Neurol.* **46**, 806–815 (1999).

43. Li, X., Overton, I. M., Baines, R. A., Keegan, L. P. & O'Connell, M. A. The ADAR RNA editing enzyme controls neuronal excitability in Drosophila melanogaster. *Nucleic Acids Res.* **42**, 1139–1151 (2014).

44. Keegan, L. P. *et al.* Functional conservation in human and Drosophila of Metazoan ADAR2 involved in RNA editing: loss of ADAR1 in insects. *Nucleic Acids Res.* **39**, 7249–7262 (2011).

45. Khan, A. *et al.* Membrane and synaptic defects leading to neurodegeneration in Adar mutant Drosophila are rescued by increased autophagy. *BMC Biol.* **18**, 15 (2020).

46. Robinson, J. E., Paluch, J., Dickman, D. K. & Joiner, W. J. ADAR-mediated RNA editing suppresses sleep by acting as a brake on glutamatergic synaptic plasticity. *Nat. Commun.* **7**, 10512 (2016).

47. St Laurent, G. *et al.* Genome-wide analysis of A-to-I RNA editing by single-molecule sequencing in Drosophila. *Nat. Struct. Mol. Biol.* **20**, 1333–1339 (2013).

48. Stapleton, M. *et al.* A Drosophila full-length cDNA resource. *Genome Biol.* **3**, RESEARCH0080 (2002).

49. Rodriguez, J., Menet, J. S. & Rosbash, M. Nascent-seq indicates widespread cotranscriptional RNA editing in Drosophila. *Mol. Cell* **47**, 27–37 (2012).

50. Ramaswami, G. *et al.* Identifying RNA editing sites using RNA sequencing data alone. *Nat. Methods* **10**, 128–132 (2013).

51. Harris, K. P. & Littleton, J. T. Transmission, development, and plasticity of synapses. *Genetics* **201**, 345–375 (2015).

52. Aponte-Santiago, N. A., Ormerod, K. G., Akbergenova, Y. & Littleton, J. T. Synaptic plasticity induced by differential manipulation of tonic and phasic motoneurons in drosophila. *J. Neurosci.* **40**, 6270–6288 (2020).

53. Pérez-Moreno, J. J. & O'Kane, C. J. GAL4 drivers specific for type ib and type is motor neurons in drosophila. *G3 (Bethesda)* **9**, 453–462 (2019).

54. Maldonado, C., Alicea, D., Gonzalez, M., Bykhovskaia, M. & Marie, B. Adar is essential for optimal presynaptic function. *Mol. Cell. Neurosci.* **52**, 173–180 (2013).

55. He, K. *et al.* Physiologic and nanoscale distinctions define glutamatergic synapses in tonic vs phasic neurons. *J. Neurosci.* **43**, 4598–4611 (2023).

56. Sauvola, C. W., Akbergenova, Y., Cunningham, K. L., Aponte-Santiago, N. A. & Littleton, J. T. The decoy SNARE Tomosyn sets tonic versus phasic release properties and is required for homeostatic synaptic plasticity. *eLife* **10**, (2021).

57. Kurdyak, P., Atwood, H. L., Stewart, B. A. & Wu, C. F. Differential physiology and morphology of motor axons to ventral longitudinal muscles in larval Drosophila. *J. Comp. Neurol.* **350**, 463–472 (1994).

58. Medeiros, A. T., Gratz, S. J., Delgado, A., Ritt, J. T. & O'Connor-Giles, K. M. Molecular and organizational diversity intersect to generate functional synaptic heterogeneity within and between excitatory neuronal subtypes. (2023) doi:10.7554/eLife.88412.1.

59. Lnenicka, G. A. & Keshishian, H. Identified motor terminals in Drosophila larvae show distinct differences in morphology and physiology. *J. Neurobiol.* **43**, 186–197 (2000).

60. Genç, Ö. & Davis, G. W. Target-wide Induction and Synapse Type-Specific Robustness of Presynaptic Homeostasis. *Curr. Biol.* **29**, 3863-3873.e2 (2019).

61. Jetti, S. K. *et al.* Molecular logic of synaptic diversity between Drosophila tonic and phasic motoneurons. *Neuron* **111**, 3554-3569.e7 (2023).

62. Newman, Z. L. *et al.* Input-Specific Plasticity and Homeostasis at the Drosophila Larval Neuromuscular Junction. *Neuron* **93**, 1388-1404.e10 (2017).

63. Aponte-Santiago, N. A. & Littleton, J. T. Synaptic properties and plasticity mechanisms of invertebrate tonic and phasic neurons. *Front. Physiol.* **11**, 611982 (2020).

64. Pecori, R., Di Giorgio, S., Paulo Lorenzo, J. & Nina Papavasiliou, F. Functions and consequences of AID/APOBEC-mediated DNA and RNA deamination. *Nat. Rev. Genet.* **23**, 505–518 (2022).

65. Bhakta, S. & Tsukahara, T. C-to-U RNA Editing: A Site Directed RNA Editing Tool for Restoration of Genetic Code. *Genes* **13**, (2022).

66. Gott, J. M. & Emeson, R. B. Functions and mechanisms of RNA editing. *Annu. Rev. Genet.* **34**, 499–531 (2000).

67. McCown, P. J. *et al.* Naturally occurring modified ribonucleosides. *Wiley Interdiscip. Rev. RNA* **11**, e1595 (2020).

68. Jacquemyn, J. *et al.* Torsin and NEP1R1-CTDNEP1 phosphatase affect interphase nuclear pore complex insertion by lipid-dependent and lipid-independent mechanisms. *EMBO J.* **40**, e106914 (2021).

69. Huntwork, S. & Littleton, J. T. A complexin fusion clamp regulates spontaneous neurotransmitter release and synaptic growth. *Nat. Neurosci.* **10**, 1235–1237 (2007).

70. Jorquera, R. A., Huntwork-Rodriguez, S., Akbergenova, Y., Cho, R. W. & Littleton, J. T. Complexin controls spontaneous and evoked neurotransmitter release by regulating the timing and properties of synaptotagmin activity. *J. Neurosci.* **32**, 18234–18245 (2012).

71. Buhl, L. K. *et al.* Differential regulation of evoked and spontaneous neurotransmitter release by C-terminal modifications of complexin. *Mol. Cell. Neurosci.* **52**, 161–172 (2013).

72. Beck, E. S. *et al.* Regulation of Fasciclin II and synaptic terminal development by the splicing factor beag. *J. Neurosci.* **32**, 7058–7073 (2012).

73. Ulrich, A. K. C., Schulz, J. F., Kamprad, A., Schütze, T. & Wahl, M. C. Structural basis for the functional coupling of the alternative splicing factors smu1 and RED. *Structure* **24**, 762–773 (2016).

74. Saoura, M., Pinnock, K., Pujantell-Graell, M. & Levinger, L. Substitutions in conserved regions preceding and within the linker affect activity and flexibility of tRNase ZL, the long form of tRNase Z. *PLoS ONE* **12**, e0186277 (2017).

75. Labrousse, A. M., Zappaterra, M. D., Rube, D. A. & van der Bliek, A. M. C. elegans dynamin-related protein DRP-1 controls severing of the mitochondrial outer membrane. *Mol. Cell* **4**, 815–826 (1999).

76. Alexander, C. *et al.* OPA1, encoding a dynamin-related GTPase, is mutated in autosomal dominant optic atrophy linked to chromosome 3q28. *Nat. Genet.* **26**, 211–215 (2000).

77. Newman, Z. L. *et al.* Determinants of synapse diversity revealed by super-resolution quantal transmission and active zone imaging. *Nat. Commun.* **13**, 229 (2022).

78. Windner, S. E., Manhart, A., Brown, A., Mogilner, A. & Baylies, M. K. Nuclear Scaling Is Coordinated among Individual Nuclei in Multinucleated Muscle Fibers. *Dev. Cell* **49**, 48-62.e3 (2019).

79. Xu, W., Biswas, J., Singer, R. H. & Rosbash, M. Targeted RNA editing: novel tools to study post-transcriptional regulation. *Mol. Cell* **82**, 389–403 (2022).

80. Christofi, T. & Zaravinos, A. RNA editing in the forefront of epitranscriptomics and human health. *J. Transl. Med.* **17**, 319 (2019).

81. Zhang, D., Zhu, L., Gao, Y., Wang, Y. & Li, P. RNA editing enzymes: structure, biological functions and applications. *Cell Biosci.* **14**, 34 (2024).

82. Ashley, J. *et al.* Retrovirus-like Gag Protein Arc1 Binds RNA and Traffics across Synaptic Boutons. *Cell* **172**, 262-274.e11 (2018).

83. van Swinderen, B. & Greenspan, R. J. Flexibility in a gene network affecting a simple behavior in Drosophila melanogaster. *Genetics* **169**, 2151–2163 (2005).

84. Littleton, J. T. *et al.* Temperature-sensitive paralytic mutations demonstrate that synaptic exocytosis requires SNARE complex assembly and disassembly. *Neuron* **21**, 401–413 (1998).

85. Ingleby, L., Maloney, R., Jepson, J., Horn, R. & Reenan, R. Regulated RNA editing and functional epistasis in Shaker potassium channels. *J. Gen. Physiol.* **133**, 17–27 (2009).

86. Liu, J., Zheng, C. & Duan, Y. New comparative genomic evidence supporting the proteomic diversification role of A-to-I RNA editing in insects. *Mol. Genet. Genomics* **299**, 46 (2024).

87. Duan, Y. *et al.* Differential adaptive RNA editing signals between insects and plants revealed by a new measurement termed haplotype diversity. *Biol. Direct* **18**, 47 (2023).

88. Pooryasin, A. *et al.* Unc13A and Unc13B contribute to the decoding of distinct sensory information in Drosophila. *Nat. Commun.* **12**, 1932 (2021).

89. Reddy-Alla, S. *et al.* Stable positioning of unc13 restricts synaptic vesicle fusion to defined release sites to promote synchronous neurotransmission. *Neuron* **95**, 1350-1364.e12 (2017).

90. Hantak, M. P., Einstein, J., Kearns, R. B. & Shepherd, J. D. Intercellular communication in the nervous system goes viral. *Trends Neurosci.* **44**, 248–259 (2021).

91. Erlendsson, S. *et al.* Structures of virus-like capsids formed by the Drosophila neuronal Arc proteins. *Nat. Neurosci.* **23**, 172–175 (2020).

92. Salter, J. D., Bennett, R. P. & Smith, H. C. The APOBEC protein family: united by structure, divergent in function. *Trends Biochem. Sci.* **41**, 578–594 (2016).

93. Bourara, K., Litvak, S. & Araya, A. Generation of G-to-A and C-to-U changes in HIV-1 transcripts by RNA editing. *Science* **289**, 1564–1566 (2000).

94. Sharma, P. M., Bowman, M., Madden, S. L., Rauscher, F. J. & Sukumar, S. RNA editing in the Wilms' tumor susceptibility gene, WT1. *Genes Dev.* **8**, 720–731 (1994).

Figure Legends

Fig. 1. RNA editing in larval motoneurons occurs primarily in mRNA coding regions and displays variable editing rates per target site. A. Schematic of canonical RNA editing where ADAR deaminates an adenosine, forming an inosine, which is interpreted as guanosine by translation machinery. RNA editing in exons can cause a missense mutation. **B.** RNA edits (blue nucleotides) were identified by comparing sequenced DNA and RNA for mismatches. Single nucleotide polymorphisms (SNPs, orange nucleotides) were filtered from the data. Grey and black horizontal bars represent DNA and RNA sequencing reads aligned to the reference genome. **C.** Ib- or Is-specific Gal4 drivers were used to express UAS-GFP to label the cells in the 3rd instar ventral nerve cord. Cells were individually patched and their RNA extracted for single cell RNA sequencing. Genomic DNA from the parental Gal4 and UAS lines were DNA sequenced. Variants were called using the Genome Analysis Toolkit (GATK) and SAMTools, with the intersection of the variants identified as potential RNA edits. Potential RNA edits were further filtered by read depth, editing percentage, and number of cells using a custom MATLAB code to result in a final list of high confidence edit sites. **D.** Among the 1637 high confidence edit sites, 316 were canonical A-to-G edits. C-to-T and G-to-A editing was also abundant. **E.** The majority of editing sites are localized in the mRNA CDS region. **F.** Edits found in the CDS had a higher average editing rate, than those in the 5'UTR or 3'UTR. Each dot represents mean editing of Ib or Is cells at a single genomic location. **G.** The frequency distribution of missense mutations from canonical editing in Ib and Is motoneurons is shown.

Fig. 2. The most highly edited targets include mRNA encoding neuronal and synaptic proteins. A. The 20 genes with the most editing sites are enriched for those regulating excitability and neurotransmission. **B.** Distribution of the frequency of edits across the neuronal population sampled. **C.** The top 20 edits that were most frequently identified in cells are shown. **D.** Distribution of edits based on proximity to other editing sites (blue histogram) with the cumulative probability density denoted (orange line).

Fig. 3. Location of selected missense RNA edits altering conserved residues within ion channels and signaling proteins. AlphaFold predicted structures with RNA edit locations marked

for selected postsynaptic receptors (**A, B, C**), excitability proteins (D, E, F), and Bsk (**G**), Beag (**H**), and RNaseZ (**I**). Color indicates model confidence at individual residues: dark blue (very high), light blue (high), yellow (low), and orange (very low). The N-terminus (N) and C-terminus (C) are denoted for each protein.

Fig. 4. Adar activity becomes rate-limiting for abundant mRNA transcripts. A. *Adar* transcript expression levels for individual Ib and Is neurons are plotted and were not significantly different. **B.** *Adar* expression did not correlate with editing level. Genes in the top 30% of transcript expression levels are shown in red. **C.** RNA editing level at single sites is inversely correlated with the mRNA expression level of the target gene for both Ib and Is neurons. **D.** Distribution of the editing rate for each individual target site (single dots) arranged in columns corresponding to the individual neuron. Neurons are ordered from lowest to highest average editing level per cell within the Ib and Is subtypes. Color denotes the density of dots in the graph, where warm colors indicate high density and cool colors low density. Single cells did not edit all sites in their transcriptome equally. Rather, target sites within a single cell were edited at levels spanning from the 10% threshold to 100% edited. **E.** There was an inverse correlation between the number of edits in a given cell and mean editing level, consistent with a model where ADAR becomes rate limiting for abundant mRNAs. Each dot represents a single cell. **F.** Editing level is inversely correlated with the fraction of cells containing the edit. **G.** Variability in editing levels for three Cpx sites highlighting cells with completely unedited (red columns), partially edited (blue and red columns), or fully edited (blue columns) transcript. Each column represents a single cell, and column order is held constant in each subplot to highlight how editing in neighboring genomic locations can vary within a single cell. White columns represent cells lacking enough reads at the site for analysis.

Fig. 5. Editing targets and editing rate is similar across Ib and Is motoneuron subtypes. A. Average RNA editing level between Ib and Is neurons was not significantly different. **B.** Levels of Ib and Is RNA editing at individual sites was highly correlated. Dots along the axes are from sites with editing in one cell type but not the other. **C.** The fraction of Ib or Is cells expressing a given edit was highly correlated. Color indicates the difference in editing rate for each edit, with warm colors representing a higher editing rate in Ib and cooler colors a higher editing rate in Is.

D. Edit sites are graphed according to differences in gene expression and RNA editing level between Ib and Is. A few edits were in differentially expressed genes (dots spread horizontally), but most genes had relatively little mRNA expression differences (dots clustered near 0 transcripts per million (TPMs)). Genes with significant differences between Ib and Is RNA editing levels (dots spread vertically), but non-significant gene-level expression differences are highlighted in red. **E.** 26 RNA editing sites (red dots in 5D) displayed statistically significant RNA editing differences between Ib and Is that did not represent DEGs. The mean RNA editing level (left side) is contrasted with gene expression level (right side) for several representative edit sites. Statistical significance for RNA editing and gene expression level is shown to the left and right of each edit site, respectively.

Fig. 6. Larval muscles edit fewer targets and have a lower editing rate than motoneurons. A. Muscle cells uniquely edit 7 sites, while 30 sites are also found in Ib or Is neurons. **B.** Muscles generally had a lower editing rate than Ib or Is neurons at sites edited in both cell types.

Table 1. Canonical RNA edits altering conserved amino acids in target proteins.
The canonical RNA edit sites that caused significant missense mutations and altered a conserved amino acid across other insect or mammalian homologs.

Supplemental Material

Supplemental Fig. 1. Non-canonical editing is not enriched for neuron-specific genes and causes more silent changes than canonical editing. A. The editing rate across 5'UTR, CDS, and 3'UTR was similar to canonical editing. **B.** The fraction of edits in the 5'UTR, CDS, and 3'UTR was similar to canonical editing. **C.** The fraction of RNA edits resulting in silent amino acid mutations was much higher for non-canonical editing (70%) than canonical editing (42%). **D.** The distribution of amino acid substitutions caused by non-canonical editing. **E.** Unlike canonical editing, genes with the most non-canonical edit sites were not enriched for neuronal genes. **F.** The average number of cells a non-canonical edit was identfied in was similar to that observed with canonical editing. **G.** Similar to canonical editing, non-canonical edits were more likely to be found near other non-canonical editing sites.

Supplemental Fig. 2. Non-canonical editing is similar across Ib and Is neurons and displays variable editing rates and a rate-limiting machinery for abundant mRNAs. A. Non-canonical editing rate is inversely proportional to the expression level of the edited gene for both Ib and Is neurons. **B.** Neurons with fewer non-canonical editing sites had a higher mean editing rate. **C.** Single neurons expressed non-canonical edits with a wide range of editing levels, although mean non-canonical editing rate (red line) was more homogenous than canonical editing (Fig. 4D). **D.** Average non-canonical RNA editing level between Ib and Is neurons was not significantly different. **E.** Levels of Ib and Is non-canonical RNA editing at individual sites was highly correlated. Dots along the axes are from sites with editing in one cell type but not the other. **F.** The fraction of Ib and Is cells expressing each non-canonical edit was highly correlated.

Supplemental Table 1: Canonical RNA (A-to-I) editing sites identified across all individual Ib motoneurons, Is motoneurons and abdominal muscles of 3rd instar larvae.

Supplemental Table 2: Summary of canonical RNA editing sites identified in Ib motoneurons, Is motoneurons and abdominal muscles.

Supplemental Table 3: Non-canonical RNA (non-A-to-I) editing sites identified across all individual Ib motoneurons, Is motoneurons and abdominal muscles of 3rd instar larvae.

Supplemental Table 4: Summary of non-canonical RNA editing sites identified in Ib motoneurons, Is motoneurons and abdominal muscles.

Supplemental Table 5: Canonical RNA editing targets with the highest editing rate that cause amino acid substitutions.

Supplemental Table 6: Canonical RNA editing site differences in Ib versus Is motoneurons following removal of differentially expressed genes (DEGs).

Supplemental Table 7: Canonical RNA editing sites identified in larval abdominal muscles.

Supplemental Item 1: Zip file of MATLAB code for RNA editing detection. This file contains the necessary MATLAB codes to process output of GATK/SAMtools variant callers as described in methods.

Table 1. Canonical Edits Altering Conserved Amino Acids

Gene	Flybase ID	Edit Position	Previously Known RNA editing	Pfam Domain	Edit site conservat	Original Codo	Edited Codon	Original AA	Edited AA	Gene function
Membrane Excitability										
qvr	FBgn0260499	2R:11447607	Yes	QVR	Insects	AGT	GGT	S	G	Regulates K^+ channels
Shab	FBgn0262593	3L:2925255	Yes	T1-type_BTB	Insects	AGT	GGT	S	G	K^+ channel
Shab	FBgn0262593	3L:2941312	Yes	Ion_trans_dom	Mammals	ACA	GCA	T	A	K^+ channel
Shab	FBgn0262593	3L:2941364	Yes	Ion_trans_dom	Mammals	TAT	TGT	Y	C	K^+ channel
Shab	FBgn0262593	3L:2941396	Yes	Ion_trans_dom	Insects	ACT	GCT	T	A	K^+ channel
CG1090	FBgn0037238	3R:4365385	Yes	NaCa_Exmemb	Mammals	AGC	GGC	S	G	Na^+/Ca^{2+} (NCX) exchange
Atpalpha	FBgn0002921	3R:20964328	Yes	-	Mammals	GAG	GGG	E	G	Na^+ pump
Atpalpha	FBgn0002921	3R:20965039	Yes	-	Insects	TAC	TGC	Y	C	Na^+ pump
slo	FBgn0003429	3R:24675663	Yes	Ion_trans_dom	Mammals	AAT	GAT	N	D	K^+ channel
OtopLa	FBgn0259994	X:5631048	Yes	Otopetrin	Insects	ACT	GCT	T	A	Proton (H^+) channel
para	FBgn0285944	X:16464719	Yes	Ion_trans_dom	Insects	AAC	AGC	N	S	Na^+ channel
para	FBgn0285944	X:16482682	Yes	Ion_trans_dom	Insects	AAT	GAT	N	D	Na^+ channel
Sh	FBgn0003380	X:17930658	Yes	-	Mammals	ACG	GCG	T	A	K^+ channel
Presynaptic Function										
cpx	FBgn0041605	3R:4297517	Yes	Synaphin	Mammals	AAT	GAT	N	D	SV exocytosis
cpx	FBgn0041605	3R:4297518	Yes	Synaphin	Mammals	AAT	AGT	N	S	SV exocytosis
lap	FBgn0086372	3R:7192775	Yes	-	Insects	ACA	GCA	T	A	SV endocytosis
Rbp	FBgn0262483	3R:15399446	Yes	-	Insects	ACC	GCC	T	A	AZ protein
Rim	FBgn0053547	3R:17881419	No	-	Insects	AGA	GGA	R	G	AZ protein
EndoA	FBgn0038659	3R:18907675	Yes	BAR_dom	Mammals	AAG	GAG	K	E	SV endocytosis
VhaAC45RP	FBgn0051030	3R:30165949	No	-	Insects	GAG	GGG	E	G	Part of SV proton pump
cac	FBgn0263111	X:11971853	Yes	Ion_trans_dom	Insects	AGT	GGT	S	G	Ca^{2+} channel
Postsynaptic Function										
nAChRalpha6	FBgn0032151	2L:9809349	Yes	Neur_chan_lig-bd	Insects	AAC	AGC	N	S	nAch receptor
nAChRalpha6	FBgn0032151	2L:9809350	Yes	Neur_chan_lig-bd	Insects	AAC	GAC	N	D	nAch receptor
nAChRalpha5	FBgn0028875	2L:14089204	Yes	Neurotrans-gated_c	Mammals	ACA	GCA	T	A	nAch receptor
Prosap	FBgn0040752	2R:14062651	Yes	-	Insects	CAG	CGG	Q	R	Shank - PSD protein
nAChRbeta1	FBgn0000038	3L:4432487	Yes	Neur_chan_lig-bd	Insects	AGA	GGA	R	G	nAch receptor
Cell Metabolism										
CG1265	FBgn0035517	3L:4255132	No	-	Mammals	GAG	GGG	E	G	Lysosomal Solute Transporter
Cell Signaling										
bsk	FBgn0000229	2L:10248292	No	Prot_kinase_dom	Mammals	GAC	GGC	D	G	JNK protein kinase
CalpB	FBgn0025866	3L:9892134	Yes	-	Mammals	AAT	AGT	N	S	Ca^{2+}-activated protease
Cytoskeletal or Cell-Cell Adhesion										
betaTub56D	FBgn0284243	2R:19447593	No	-	Mammals	GAC	GGC	D	G	Tubulin component
CG13506	FBgn0034723	2R:22391510	Yes	-	Insects	CAG	CGG	Q	R	Ig domain protein
CG32264	FBgn0052264	3L:3717400	No	-	Mammals	AGG	GGG	R	G	Role in actin biology
Membrane Trafficking										
Snx21	FBgn0031457	2L:2764358	No	-		GAG	GGG	E	G	Sorting Nexin
Sec23	FBgn0262125	3R:5650231	Yes	Sec23/24_trunk_do	Mammals	CAG	CGG	Q	R	COPII component in ER-Golgi transport
Sec23	FBgn0262125	3R:5650351	Yes	Sec23/24_trunk_do	Mammals	CAG	CGG	Q	R	COPII component in ER-Golgi transport
CG42613	FBgn0261262	3R:18969789	No	CUB_dom	Insects	GAT	GGT	D	G	Plasma membrane protein
Mitochondrial Function										
muc	FBgn0283658	2L:7429847	No	2-oxoacid_DH_acty	Mammals	GAG	GGG	E	G	Component of mitochondrial pyruvate dehydrogenase complex
Opa1	FBgn0261276	2R:14234798	No	-	Mammals	AAT	GAT	N	D	Mitochondrial dynamin
bonsai	FBgn0026261	2R:22638356	No	Ribosomal_uS15	Insects	GAC	GGC	D	G	Mitochondrial ribosomal protein
Transcription/Splicing/Nuclear Function										
RNaseZ	FBgn0028426	2R:10307375	No	-	Mammals	GAA	GGA	E	G	tRNA processing
Hr78	FBgn0015239	3L:21494397	No	Nucl_hrmn_rcpt_lig	Mammals	GAG	GGG	E	G	Nuclear Steroid Receptor
beag	FBgn0037660	3R:9063537	No	RED_C	Insects	AGC	GGC	S	G	Splicesomal component - regulates Fas2 splicing
Sxl	FBgn0264270	X:7085816	Yes	-	Insects	AGC	GGC	S	G	RNA binding protein

Figure 1

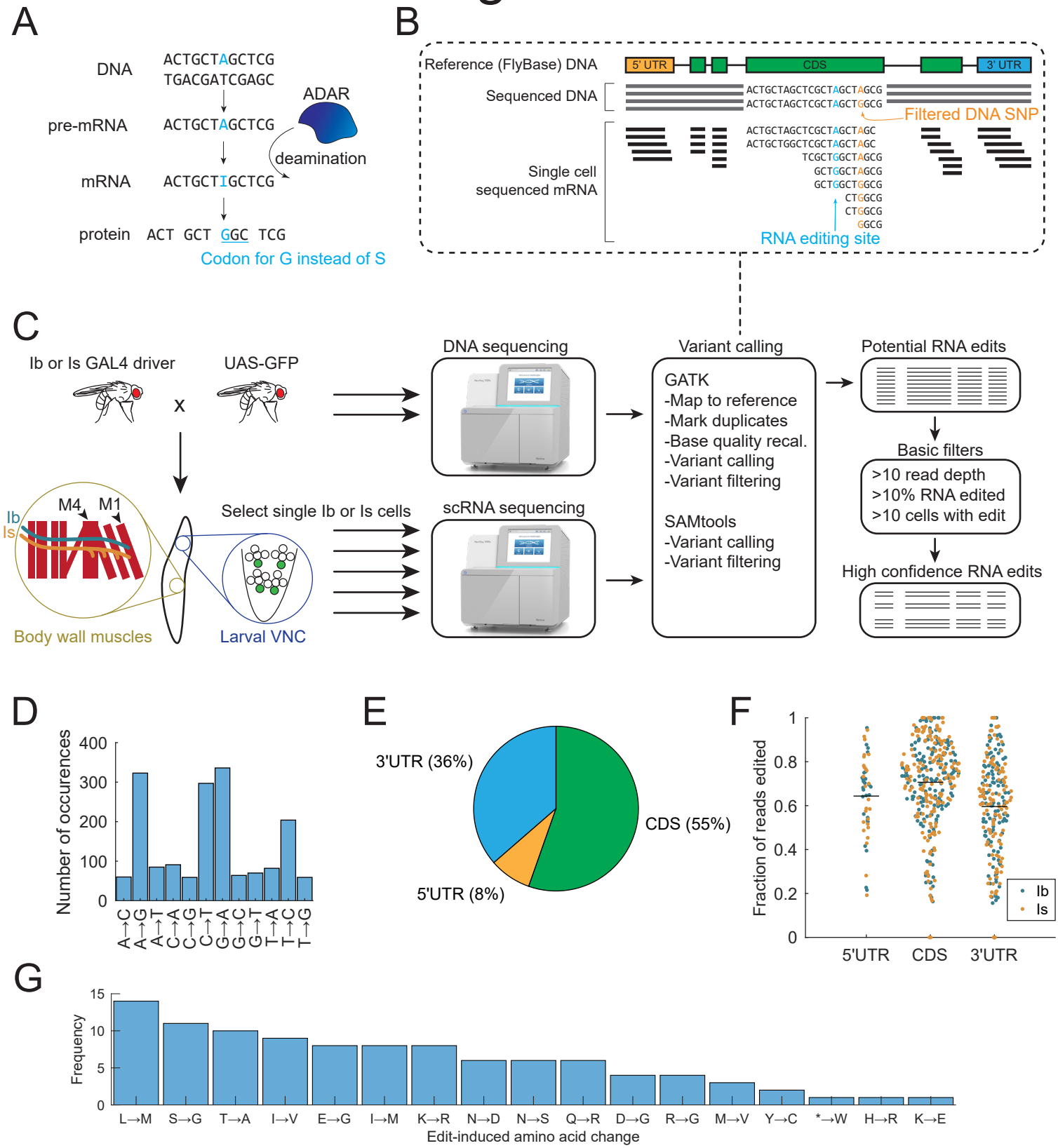
A
DNA
ACTGCTAGCTCG
TGACGATCGAGC
ADAR
pre-mRNA
ACTGCTAGCTCG
deamination
mRNA
ACTGCTIGCTCG
protein
ACT GCT GGC TCG
Codon for G instead of S
B
Reference (FlyBase) DNA
5' UTR
CDS
3' UTR
Sequenced DNA
ACTGCTAGCTCGCTAGCTAGCG
ACTGCTAGCTCGCTAGCTGGCG
Filtered DNA SNP
Single cell sequenced mRNA
ACTGCTAGCTCGCTAGCTAGC
ACTGCTGGCTCGCTAGCTAGC
TCGCTGGCTAGCG
GCTGGCTAGCG
GCTGGCTGGCG
CTGGCG
CTGGCG
GGCG
RNA editing site
C
Ib or Is GAL4 driver
x
UAS-GFP
DNA sequencing
Variant calling
Potential RNA edits
GATK
-Map to reference
-Mark duplicates
-Base quality recal.
-Variant calling
-Variant filtering
SAMtools
-Variant calling
-Variant filtering
Basic filters
>10 read depth
>10% RNA edited
>10 cells with edit
High confidence RNA edits
Ib
Is
M4
M1
Select single Ib or Is cells
scRNA sequencing
Body wall muscles
Larval VNC
D
Number of occurences
400
300
200
100
0
A→C
A→G
A→T
C→A
C→G
C→T
G→A
G→C
G→T
T→A
T→C
T→G
E
3'UTR (36%)
CDS (55%)
5'UTR (8%)
F
Fraction of reads edited
1
0.8
0.6
0.4
0.2
0
5'UTR
CDS
3'UTR
Ib
Is
G
Frequency
15
10
5
0
L→M
S→G
T→A
I→V
E→G
I→M
K→R
N→D
N→S
Q→R
D→G
R→G
M→V
Y→C
*→W
H→R
K→E
Edit-induced amino acid change

Figure 2

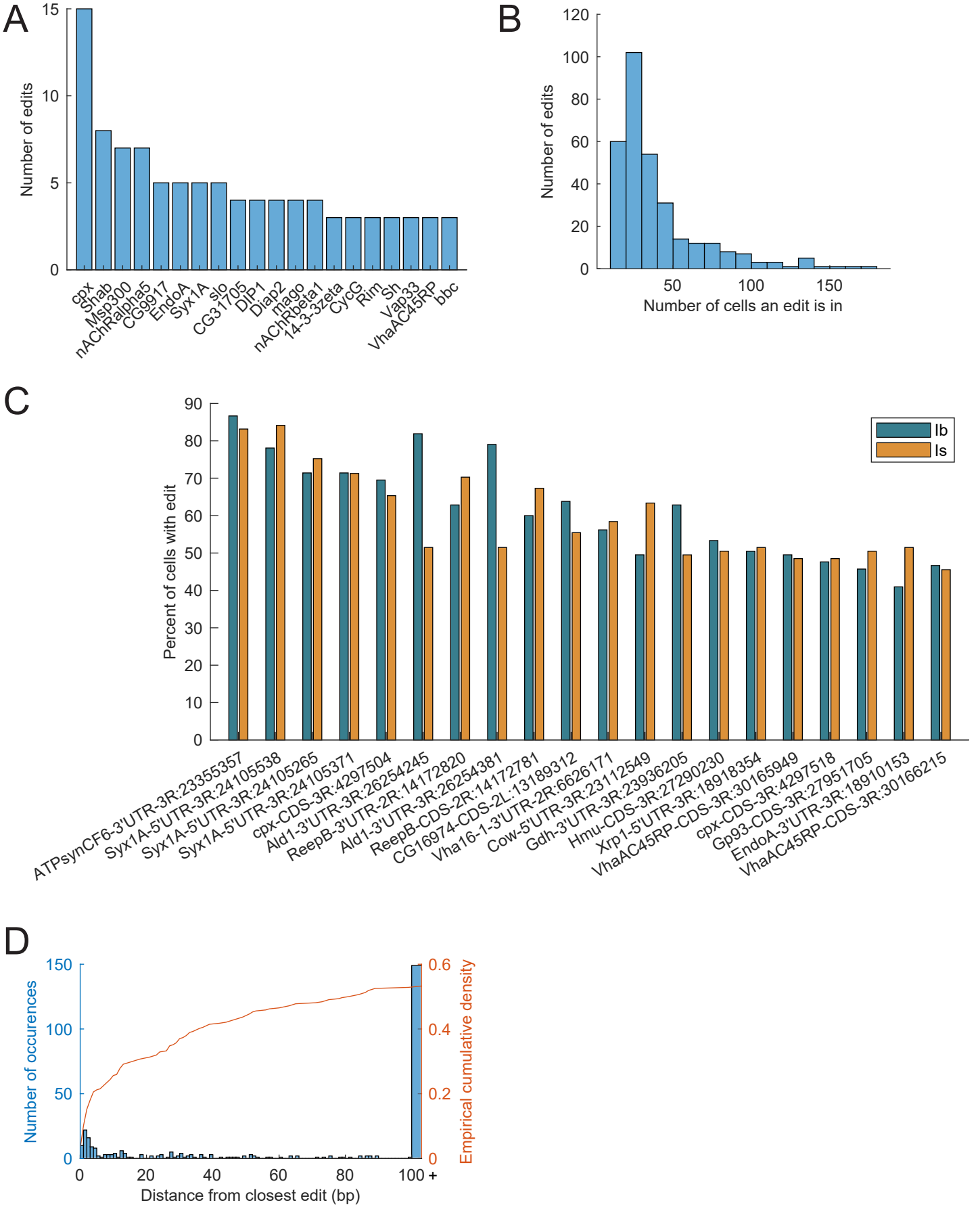
A
Number of edits
cpx
Shab
Msp300
nAChRalpha5
CG9917
EndoA
Syx1A
slo
CG31705
DIP1
Diap2
mago
nAChRbeta1
14-3-3zeta
CycG
Rim
Sh
Vap33
VhaAC45RP
bbc
B
Number of edits
Number of cells an edit is in
C
Percent of cells with edit
Ib
Is
ATPsynCF6-3'UTR-3R:23355357
Syx1A-5'UTR-3R:24105538
Syx1A-5'UTR-3R:24105265
Syx1A-5'UTR-3R:24105371
cpx-CDS-3R:4297504
Ald1-3'UTR-3R:26254245
ReepB-3'UTR-2R:14172820
Ald1-3'UTR-3R:26254381
ReepB-CDS-2R:14172781
CG16974-CDS-2L:13189312
Vha16-1-3'UTR-2R:6626171
Cow-5'UTR-3R:23112549
Gdh-3'UTR-3R:23936205
Hmu-CDS-3R:27290230
Xrp1-5'UTR-3R:18918354
VhaAC45RP-CDS-3R:30165949
cpx-CDS-3R:4297518
Gp93-CDS-3R:27951705
EndoA-3'UTR-3R:18910153
VhaAC45RP-CDS-3R:30166215
D
Number of occurences
Empirical cumulative density
Distance from closest edit (bp)

Figure 3

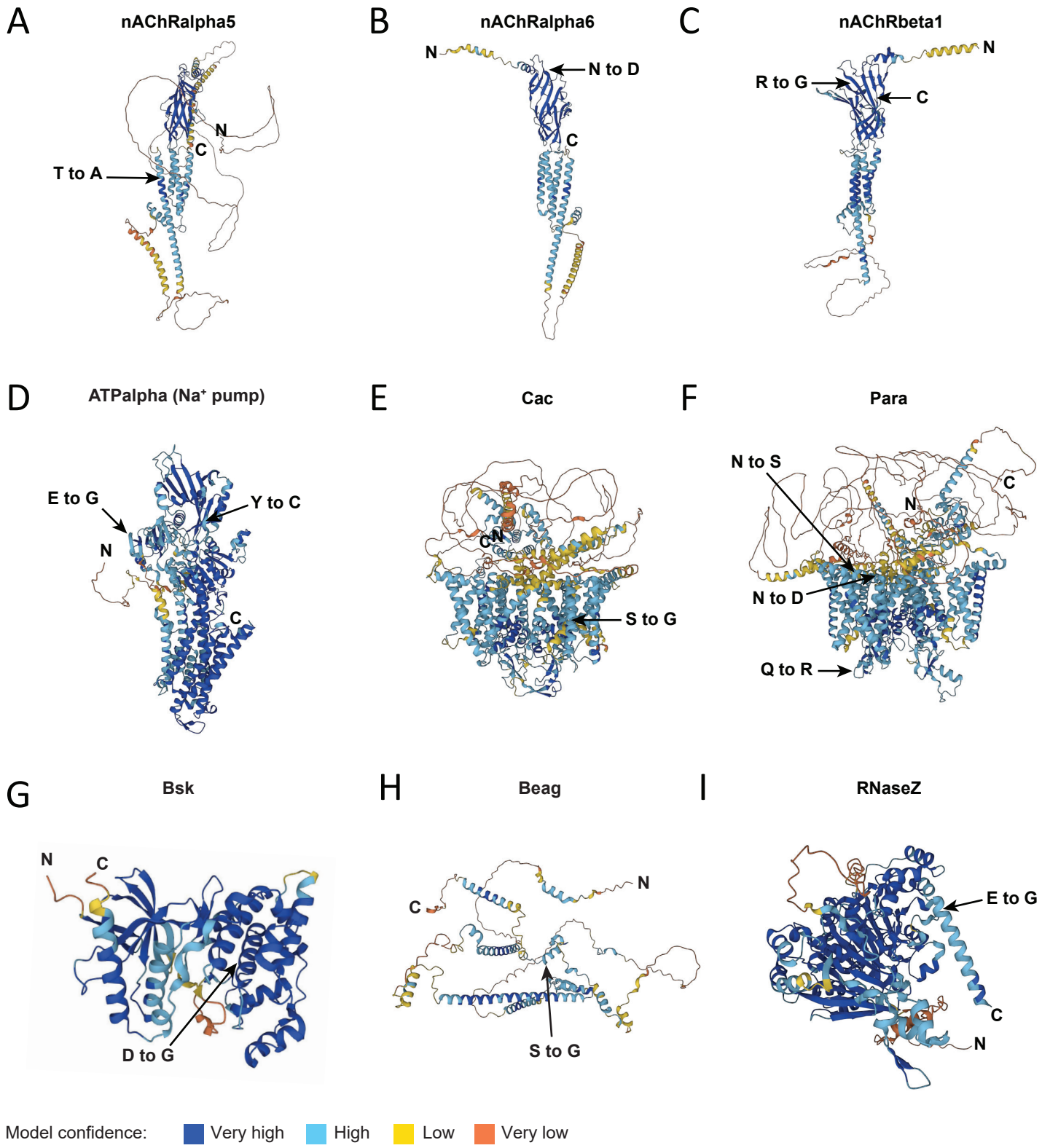

Model confidence: Very high High Low Very low

Figure 4

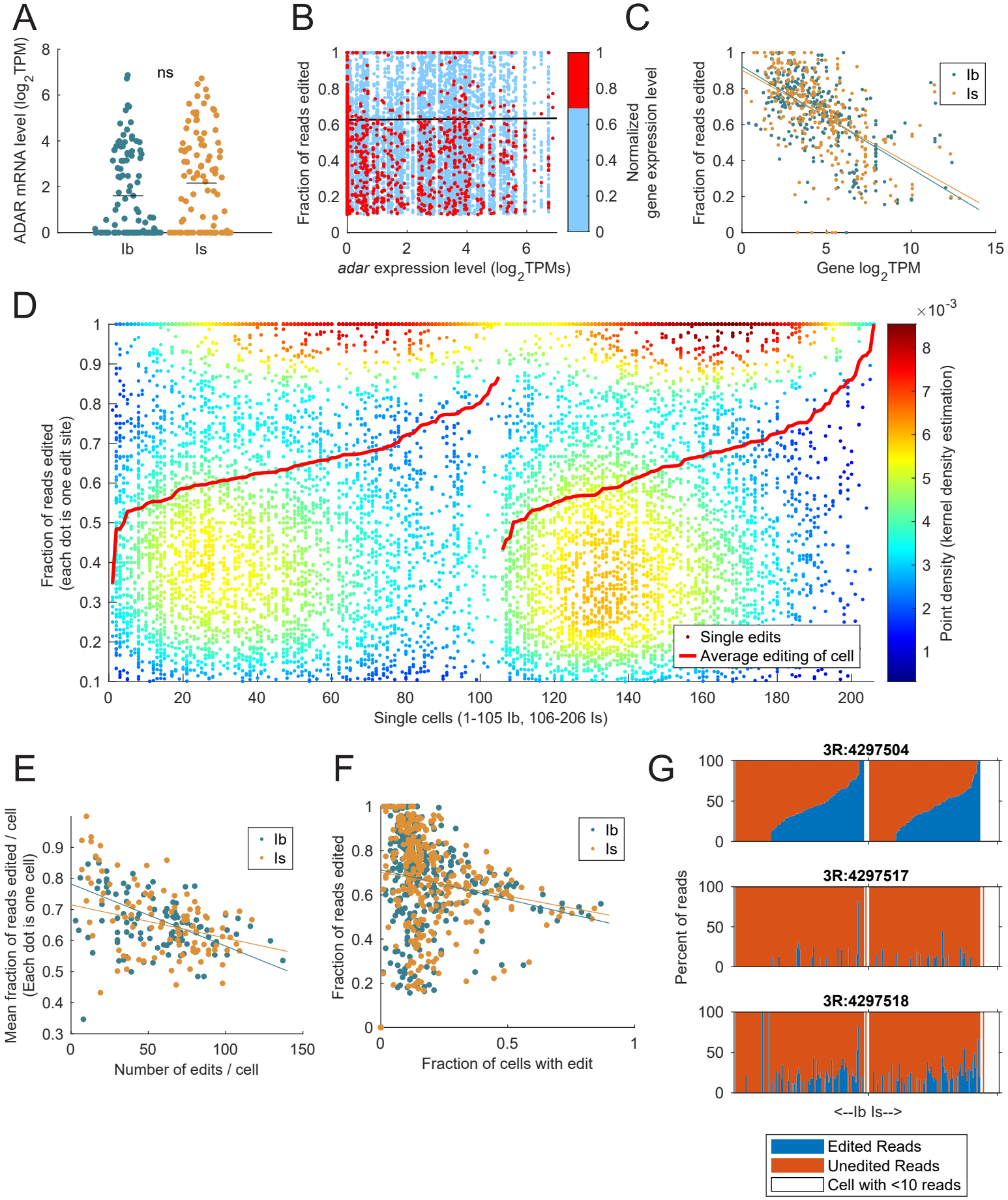
A
ADAR mRNA level (log2 TPM)
ns
Ib
Is
B
Fraction of reads edited
adar expression level (log2TPMs)
Normalized gene expression level
C
Fraction of reads edited
Gene log2TPM
Ib
Is
D
Fraction of reads edited (each dot is one edit site)
Single cells (1-105 Ib, 106-206 Is)
Single edits
Average editing of cell
Point density (kernel density estimation)
×10-3
E
Mean fraction of reads edited / cell (Each dot is one cell)
Number of edits / cell
Ib
Is
F
Fraction of reads edited
Fraction of cells with edit
Ib
Is
G
3R:4297504
3R:4297517
3R:4297518
Percent of reads
<--Ib Is-->
Edited Reads
Unedited Reads
Cell with <10 reads

Figure 5

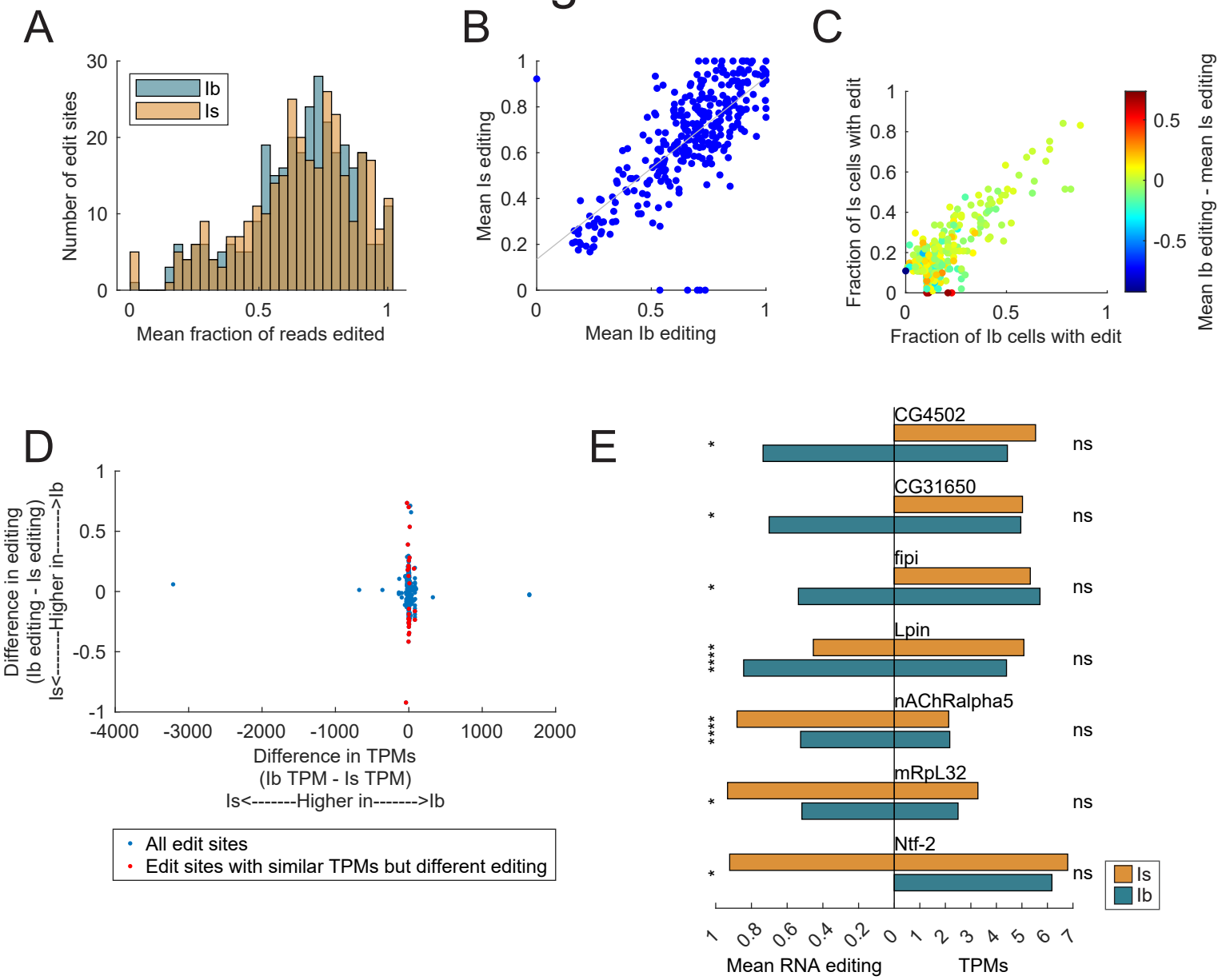
A
Ib
Is
Number of edit sites
Mean fraction of reads edited
B
Mean Is editing
Mean Ib editing
C
Fraction of Is cells with edit
Fraction of Ib cells with edit
Mean Ib editing - mean Is editing
D
Difference in editing
(Ib editing - Is editing)
Is<-------Higher in------->Ib
Difference in TPMs
(Ib TPM - Is TPM)
Is<-------Higher in------->Ib
All edit sites
Edit sites with similar TPMs but different editing
E
CG4502
CG31650
fipi
Lpin
nAChRalpha5
mRpL32
Ntf-2
ns
Is
Ib
Mean RNA editing
TPMs

Figure 6

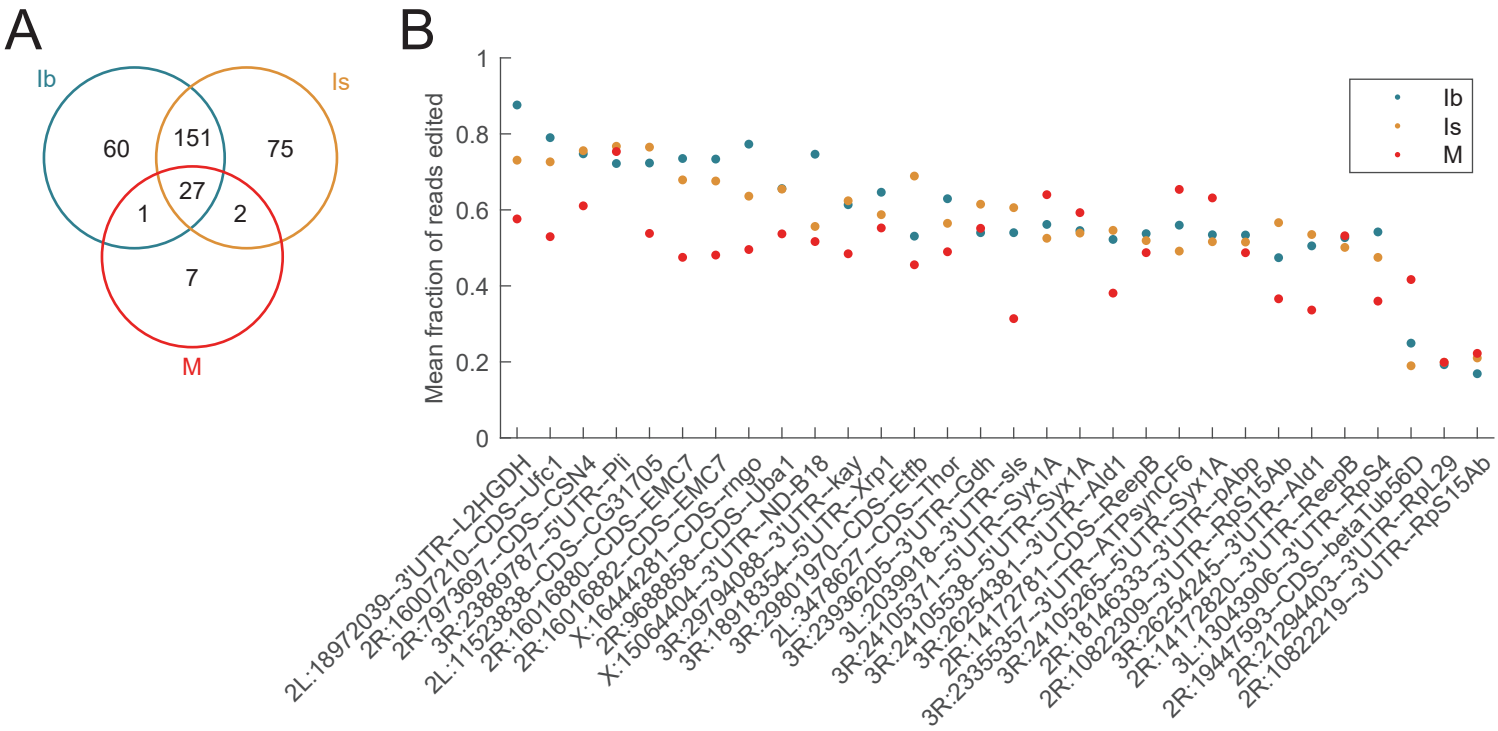
A
Ib
Is
M
60
151
75
27
1
2
7
B
Mean fraction of reads edited
0
0.2
0.4
0.6
0.8
1
Ib
Is
M
2L:18972039--3'UTR--L2HGDH
2R:16007210--CDS--Ufc1
2R:7973697--CDS--CSN4
3R:23889787--5'UTR--Pli
2L:11523838--CDS--CG31705
2R:16016880--CDS--EMC7
2R:16016882--CDS--EMC7
X:16444281--CDS--rngo
2R:9688858--CDS--Uba1
X:15064404--3'UTR--ND-B18
3R:29794088--3'UTR--kay
3R:18918354--5'UTR--Xrp1
3R:29801970--CDS--Etfb
2L:3478627--CDS--Thor
3R:23936205--3'UTR--Gdh
3L:2039918--3'UTR--sls
3R:24105371--5'UTR--Syx1A
3R:24105538--5'UTR--Syx1A
3R:26254381--3'UTR--Ald1
2R:14172781--CDS--ReepB
3R:23355357--3'UTR--ATPsynCF6
3R:24105265--5'UTR--Syx1A
2R:18146333--3'UTR--pAbp
2R:10822309--3'UTR--RpS15Ab
3R:26254245--3'UTR--Ald1
2R:14172820--3'UTR--ReepB
3L:13043906--3'UTR--RpS4
2R:19447593--CDS--betaTub56D
2R:21294403--3'UTR--RpL29
2R:10822219--3'UTR--RpS15Ab

Supplemental Figure 1

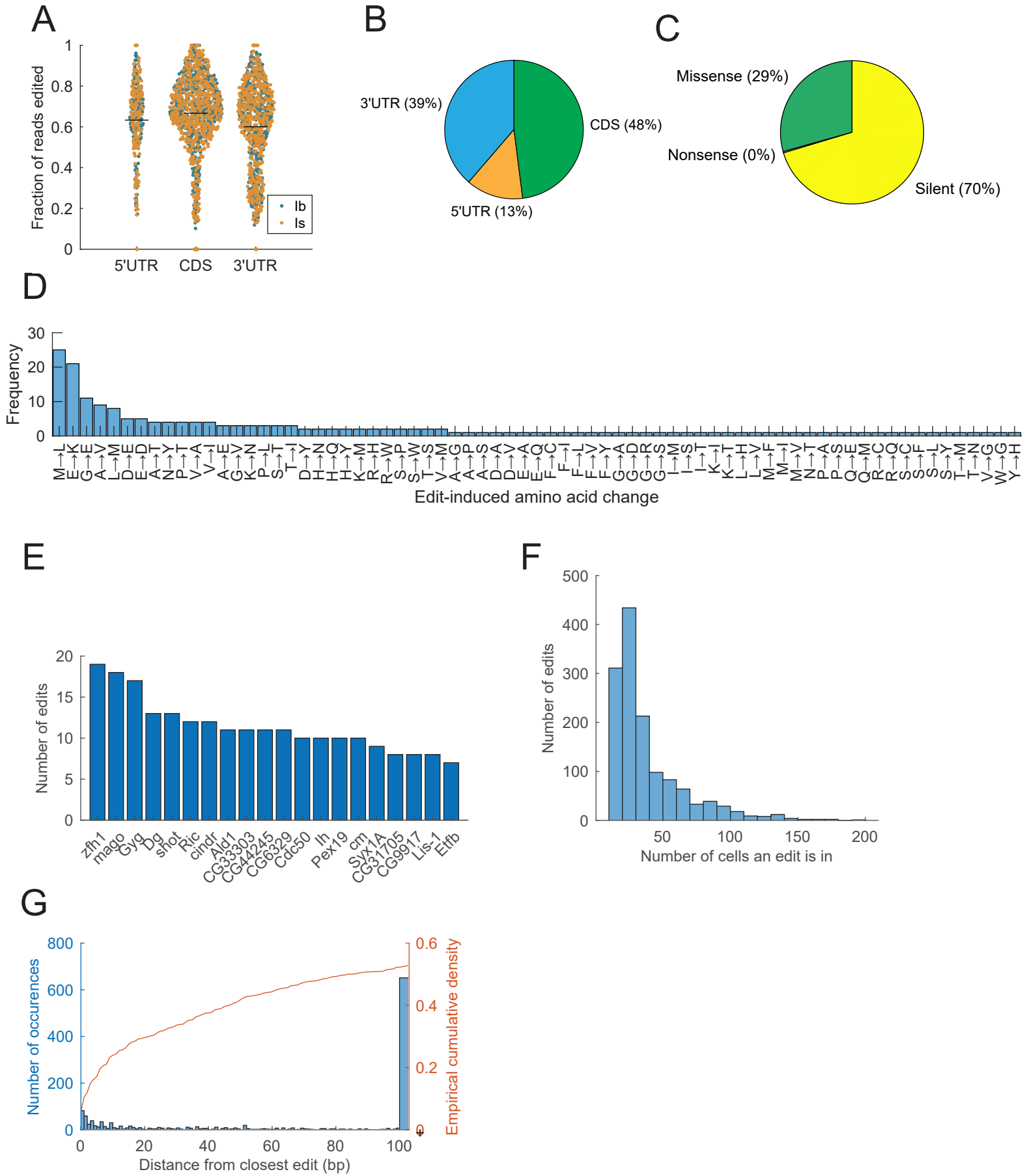
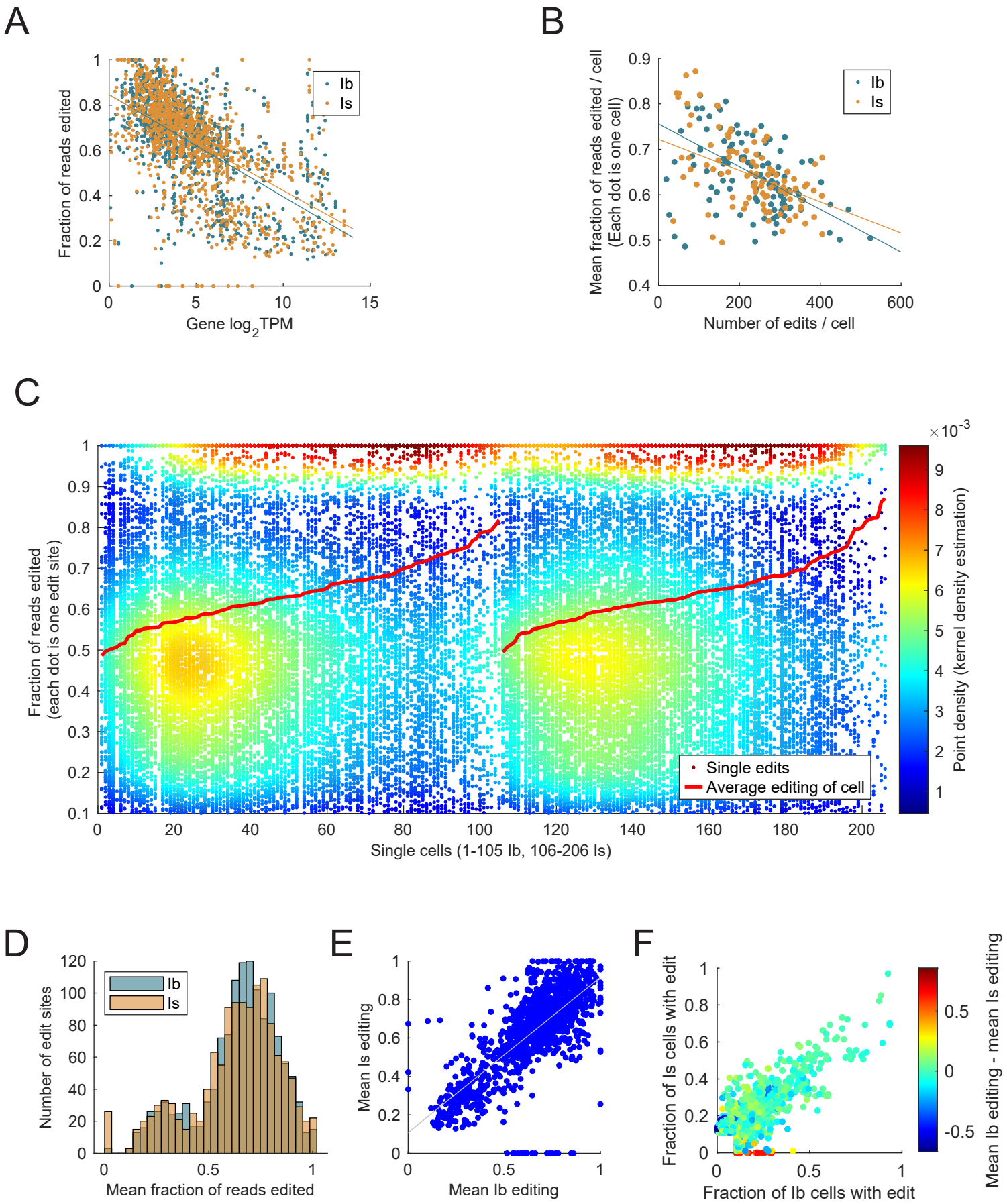
Supplemental Figure 2